

N 70 27386

NASA CR 106209

**FREQUENCY RESPONSE APPROACH TO
DESIGN OF ADAPTIVE CONTROL SYSTEMS
VIA MODEL OF SPECIFICATIONS**

by

NED TETSUYOSHI ODA

This research was sponsored by the
National Aeronautics and Space Administration
under research grant NGR 06-003-083

**CASE FILE
COPY**

DEPARTMENT OF ELECTRICAL ENGINEERING
UNIVERSITY OF COLORADO
BOULDER, COLORADO

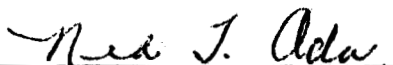
August 1, 1969

FREQUENCY RESPONSE APPROACH TO
DESIGN OF ADAPTIVE CONTROL SYSTEMS
VIA MODEL OF SPECIFICATIONS

by

Ned Tetsuyoshi Oda

This research was sponsored by the
National Aeronautics and Space Administration
under research grant NGR 06-003-083


Ned Tetsuyoshi Oda.


Isaac M. Horowitz
Research Supervisor

Department of Electrical Engineering

University of Colorado

Boulder, Colorado

August 1, 1969

FREQUENCY RESPONSE APPROACH TO
DESIGN OF ADAPTIVE CONTROL SYSTEMS
VIA MODEL OF SPECIFICATIONS

Abstract--This report presents a method of translating time domain specifications to frequency domain specifications via specification modeling. This technique is investigated for use with the "Frequency Response Approach to the Sensitivity Problem" design method presented in I. M. Horowitz' Synthesis of Feedback Systems, Academic Press, Inc., New York, N. Y. 1963.

The technique entails finding "model" time functions which bound the desired time domain specifications, taking the Laplace transform of the known functions, and then using these transforms (transfer functions) as boundary specifications in the frequency domain. The investigation and results of using this method on a second-order plant with varying parameters is shown.

ACKNOWLEDGEMENT

Grateful appreciation is given to Professor Issac M. Horowitz but for whose guidance, vast knowledge, and intensive work in this area of research this paper would not have been possible. Also, appreciation is due Don Lewis whose computer program made possible the verification of results, without which meaningful conclusions could not have been made.

TABLE OF CONTENTS

CHAPTER	PAGE
I	INTRODUCTION
1.1	Advantage of Frequency Response Approach..... 1
1.2	Problem Statement..... 1
1.3	Method of Approach..... 2
1.4	Notation Convention..... 3
1.5	Outline of Procedure for Frequency Response Design... 4
1.6	Verification Model..... 5
II	SIMPLE FIRST-ORDER MODEL
2.1	Example 1, First-order Model..... 8
2.2	Analysis..... 18
III	SECOND-ORDER MODEL
3.1	Purpose of Second-order Model..... 20
3.2	Example 2, Second-order Model Without Overshoot..... 20
3.3	Analysis of Example 2, Second-order Model Without Overshoot..... 25
3.4	Example 3, Second-order Model With 10% Allowable Overshoot..... 31
3.5	Analysis of Example 3, Second-order Model With 10% Allowable Overshoot..... 37
IV	THIRD-ORDER MODEL
4.1	Introduction..... 43
4.2	Example 4, Third-order Model With 10% Allowable Overshoot..... 43
4.3	Analysis of Example 4, Third-order Model With 10% Allowable Overshoot..... 52
V	DOMINANT POLE-ZERO DESIGN
5.1	Purpose of Investigating a Dominant Pole-Zero Design..... 58
5.2	A Dominant Pole-Zero Design..... 58
5.3	Results of Dominant Pole-Zero Design..... 65
VI	CONCLUSION
6.1	Final Analysis..... 69
	BIBLIOGRAPHY..... 72
	APPENDIX A. $P_o(j\omega_x)/P(j\omega_x)$ Data for Second-order Plant..... 73

LIST OF TABLES

TABLE		PAGE
2.1	Magnitude and Phase Ratios for Example 1.....	12
3.1	Magnitude and Phase Ratios for Example 2.....	23
3.2	Magnitude and Phase Ratios for Example 3.....	33
4.1	Magnitude and Phase Ratios for Example 4.....	46

LIST OF ILLUSTRATIONS

FIGURE		PAGE
1.1	Two-Degree-of-Freedom System.....	2
1.2	$T_o/T(jw_x) = \underline{QV/QN}$	3
1.3	Verification Model.....	6
2.1	Specification Response Curves for Example 1.....	10
2.2	Bode Plot of Specification Boundary and Model for Example 1.....	13
2.3	Complex Plane Plot of $-L_o(jw_x)$ Minimum Boundaries for Example 1.....	15
2.4	Bode Plot of $L_o(s)$ for Example 1.....	16
2.5	Two-Degree-of-Freedom System.....	17
2.6	System Response Curves for Example 1.....	19
3.1	Example of Phase Lead.....	21
3.2	Specification Response Curves for Example 2.....	22
3.3	Bode Plot of Specification Boundary and Model for Example 2.....	24
3.4a	Complex Plane Plot of $-L_o(jw_x)$ Minimum Boundaries for Example 2, Sheet 1.....	26
3.4b	Complex Plane Plot of $-L_o(jw_x)$ Minimum Boundaries for Example 2, Sheet 2.....	27
3.5	Bode Plot of $L_o(s)$ for Example 2.....	28
3.6	System Response Curves for Example 2.....	29
3.7	Dominant Pole-zero Patterns for System Responses of Example 2.....	30
3.8	Specification Response Curves for Example 3.....	32
3.9	Bode Plot of Specification Boundary and Model for Example 3.....	34
3.10a	Complex Plane Plot of $-L_o(jw_x)$ Minimum Boundaries for Example 3, Sheet 1.....	35

FIGURE		PAGE
3.10b	Complex Plane Plot of $-L_O(j\omega_x)$ Minimum Boundaries for Example 3, Sheet 2.....	36
3.11	Bode Plot of $L_O(s)$ for Example 3.....	38
3.12a	System Response Curves for Example 3, Case A.....	40
3.12b	System Response Curves for Example 3, Case B.....	41
4.1	Specification Response Curves for Example 4.....	45
4.2	Bode Plot of Specification Boundary and Model for Example 4.....	47
4.3a	Complex Plane Plot of $-L_O(j\omega_x)$ Minimum Boundaries for Example 4, Sheet 1.....	49
4.3b	Complex Plane Plot of $-L_O(j\omega_x)$ Minimum Boundaries for Example 4, Sheet 2.....	50
4.4	Bode Plot of $L_O(s)$ for Example 4.....	51
4.5a	System Response Curves for Example 4, Case A.....	55
4.5b	System Response Curves for Example 4, Case B.....	56
4.5c	System Response Curves for Example 4, Case C.....	57
5.1	Complex Plane for Dominant Pole-Zero Design.....	59
5.2	Mapping of Allowable Specification Space.....	61
5.3	Mapping Plant Variation Region.....	63
5.4	Bode Plot of $L_F(s)$ for Dominant Pole-Zero Design.....	64
5.5	System Response for Dominant Pole-Zero Design.....	66
5.6	Typical Pole-Zero Pattern of Dominant Design Transfer Function.....	67

CHAPTER I
INTRODUCTION

1.1 Advantage of Frequency Response Approach

The objective of this research is to extend the "Frequency Response Approach to the Sensitivity Problem" (Synthesis for General Plant Parameter Variations) due to Horowitz {1}, into a workable design procedure. The advantage of the frequency response method of synthesis ($L(j\omega)$ shaping) is the openness of the method. The designer can fairly simply form minimum magnitude of $L(j\omega)$ while taking into account any practical consideration in the realization of $L(s)$. He can determine the benefits of feedback {2} and consider any constraints such as stability margins on account of parameter variations. He is not limited to any particular order or form {3} of system.*

1.2 Problem Statement

In most cases, one is concerned, ultimately, with the time response of a system. Hence, it is only natural that specifications of desired response are given as time domain specifications. Herein lies the main disadvantage or problem of the frequency response approach. There is no simple, exact correlation between the frequency domain and the time domain and, hence, it is difficult to translate the time domain specification into meaningful frequency response specifications {4}.

*For comparison of Open-loop Frequency Response Method vs $T(s)$ Pole-zero Method see reference {4} of bibliography.

1.3 Method of Approach

In this research, we investigate the use of a "model" to transform time domain specifications into a set of frequency domain specifications suitable for use with frequency response synthesis of adaptive control systems. That is, given a set of time domain specifications, the designer searches for a set of time functions which bound the given specifications. Then the transfer functions of these known time functions (i.e. their Laplace transforms) are used as the boundary specifications in the frequency domain. To use the frequency response synthesis method {1}, a "model" transfer function is selected that lies within the boundary transfer functions just determined.

The frequency response synthesis method {1} (once the frequency domain specifications are known) is briefly outlined here as background material. Consider the system in figure 1.1.

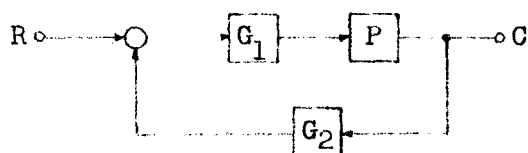


Figure 1.1 Two-degree-of-freedom system.

The transfer function

$$\begin{aligned}
 T(s) &= C(s)/R(s) \\
 &= \frac{G_1 P}{1 + G_1 G_2 P} \\
 &= \frac{G_1 P}{1 + L} \quad (1)
 \end{aligned}$$

$$\text{Where } L(s) = G_1 G_2 P, \quad (2)$$

$P(s)$ is the plant transfer function, and $G_1(s)$ and $G_2(s)$ are compensation blocks available to the designer. Now if $P(s) = P_0(s)$ (some nominal value of $P(s)$), then (1) and (2) becomes

$$\frac{G_1 P_o}{1+L_o} = T_o(s) \tag{3}$$

$$\text{and } G_1 G_2 P_o = L_o(s) \tag{4}$$

Dividing (1) into (3),

$$\frac{T_o}{T} = \frac{G_1 P_o}{1+L_o} \frac{1+L}{G_1 P} = \frac{(P_o/P)(1+L)}{1+L_o} = \frac{(P_o/P)+L_o}{1+L_o} \tag{5}$$

Suppose at $s = jw_x$, the plant parameter variations of $P_o(jw_x)/P(jw_x)$ map out an area on the complex plane as shown

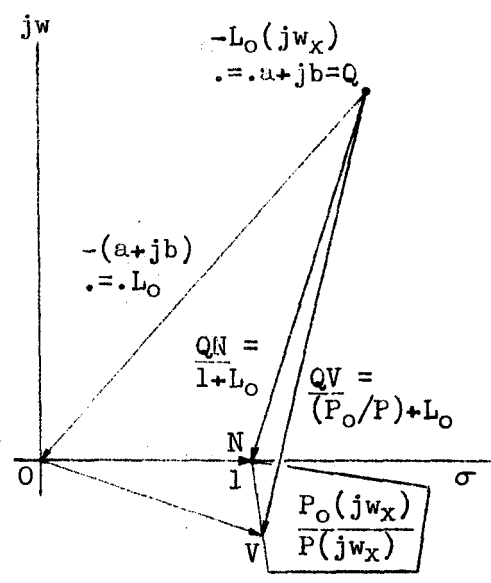


Figure 1.2 $T_o/T(jw_x) = QV/QN$

in figure 1.2.

Now if $-L_o(jw_x)$ is given by the complex number $a + jb$ located at Q then the ratio T_o/T is equal to the ratio of vectors $QV/QN = [(P_o/P) + L_o]/(1 + L_o)$, as derived in equation (5).

The range of variation of vector QV fixes the range of variation of T_o/T at $s = jw_x$, and defines a $-L_o(jw_x)$ minimum boundary $\{1\}$.

1.4 Notation Convention

The following notation is used throughout this paper.

- A, B, ... : different cases of same example.
- C, C(s) : Laplace transform of system output.
- G₁, G₁(s), H, H(s) : Laplace transform of compensation functions.
- j : imaginary number = $\sqrt{-1}$
- L, L(s) : Laplace transform of Loop transmission.

$L(j\omega)$: $L(s)$ evaluated at $s = j\omega$.
$P, P(s)$: Plant transfer function, assumed known or given.
$R, R(s)$: Laplace transform of system input, assume to be $1/s$ unless otherwise noted.
s	: Laplace complex variable = $\sigma - j\omega$
$T, T(s)$: Transfer function = C/R

Lower case letters will denote the corresponding time function, except for $T(t)$ which is defined as the time response of $T(s)$ (since t is usually understood to be time), i.e.

$T(t)$: Inverse Laplace transform of $T(s)$.
ω	: A real number defining imaginary part of Laplace complex variable s ; denotes frequency in radian-per-second.
z	: Damping factor for second-order equation; usually denoted by zeta.
ϕ_i	: Phase of appropriate s -domain function.
σ	: Real part of Laplace complex variable s .

1.5 Outline of Procedure for Frequency Response Design

In order to correlate the results of one example with those of another, an outline of the combined (in the sense that steps are due to Horowitz {1} and to considerations of section 1.3 preceding) procedure followed in this paper, is listed in reference. Details of each step is contained in the examples following or as per design techniques given in reference {1}.

Given: A plant, the range of values through which it varies, and the desired time domain specifications.

Step 1) Determine time functions which bound the given time domain specifications; take their Laplace transforms, $T(s)$ lower $\hat{=}$ T_l and $T(s)$ upper $\hat{=}$ T_u ; and plot on Bode plot.

Step 2) Pick a "model" transfer function, $T(s)$ model $\hat{=}$ T_m , whose Bode plot lies between those of T_l and T_u (i.e. $T_l \leq T_m \leq T_u$), and calculate the magnitude and phase of the ratios T_m/T_u and T_m/T_l for selected w 's $\hat{=}$ w_x , throughout the frequency range.

Note: The following steps are essentially those given in reference {1}.

Step 3) Pick a nominal value of plant transfer function, $P_o(s)$, and evaluate $P_o(jw_x)/P(jw_x)$ for bounding variations of $P(s)$. Do this for each of the previously selected w_x 's. Plot results on complex plane.

Step 4) Determine loci of $-L_o(jw_x)$ minimum boundaries on complex plane plot of step 3.

Step 5) Determine a feasible $L_o(jw)$ function from results of step 4 and consideration of magnitude and phase relationships.

Step 6) Determine suitable G_i functions for type system chosen.

1.6 Verification Model

The following two-degree-of-freedom structure is used to simulate (either by analog or digital computer) the system design for verification purposes. This particular form is used as it eliminates the need for calculating the G_i 's shown in figure 1.1.

From section 1.3, equations (3) and (4)

$$T_o(s) = \frac{G_1 P_o}{1+L_o} \quad (3)$$

$$\text{and, } L_o(s) = G_1 G_2 P_o \quad (4)$$

then if $T_o(s) = T_m$,

$$G_1 = T_m(1+L_o)/P_o \quad (6)$$

$$\text{and, } G_2 = L_o/G_1 P_o = L_o/T_m(1+L_o) \quad (7)$$

but from equation (2),

$$L = G_1 G_2 P \quad (2)$$

$$= [T_m(1+L_o)/P_o] P [L_o/T_m(1+L_o)] = PL_o/P_o$$

and from equation (5),

$$\frac{T_o}{T} = \frac{(P_o/P)+L_o}{1+L_o} \quad (5)$$

but $T_o = T_m$, therefore,

$$T = T_m(1+L_o) \frac{1}{(P_o/P)+L_o} = T_m(1+L_o) \frac{P/P_o}{1+PL_o/P_o} \quad (9)$$

and the form shown in figure 1.3, is derived

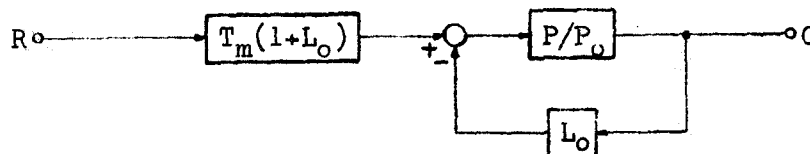


Figure 1.3 Verification Model.

In examples 2 through 4C, eighteen different parameter variation response curves ($k = 1, 2, 10$; $w_p = 1, 2, 3$; $z_p = 0.2, 0.6$) were run to verify the results of each design. However, in order to show the results on one figure, for easy comparison and analysis,

only limiting cases (maximum, minimum, worst, etc.) are shown.

For the first example, a simple plant and model will be used to clearly illustrate the steps involved.

CHAPTER 11

SIMPLE FIRST-ORDER MODEL

2.1 Example 1, First-order Model

Given: Plant transfer-function, $P(s) = K$, $1 \leq K \leq 10$, and

desired time domain specifications as follows:

Rise time, 0 to 90% : 0.55 to 1.15 seconds

Settling time, $\pm 1\%$: 1.15 to 2.30 seconds

Overshoot limit : 0%

Step 1) The desired system configuration is to be a two-degree-of-freedom system, with $G = T_m(1+L_o)/P_o$ and $H = L_o/T_m(1+L_o)$ (see step 6). From initial value theorem of Laplace transform theory {6},

$\lim_{s \rightarrow \infty} sF(s) = \lim_{t \rightarrow 0^+} f(t) = f(0^+)$. Or, for the step response of a

transfer function, we desire $\lim_{s \rightarrow \infty} F(s) = f(0^+) \equiv 0$ (no initial

condition), i.e. we desire compensation blocks which do not respond

instantaneously. Therefore, for $g(t)$ (inverse transform of $G(s)$)

to be zero at $t = 0$, requires that $G(s)$ have at least one more pole

than zeros. But $G = T_m(1+L_o)/P_o$ and $(1+L_o)$ has no excess poles,

hence T_m must have at least one more excess pole than P_o . Similarly,

for $h(t) = 0$ at $t = 0$, requires L_o to have at least one more excess

pole than T_m . Now, since the form of T_1 ($T(s)$ lower) determines the

form of T_m (see step 2), the requirements on T_m are also requirements

of T_1 , or T_1 must have at least one more pole in excess of its zeros

than P_o has. In this example, a first-order response satisfies the

requirement that the excess poles over zeros of T_1 ($e_T = 1$) be at

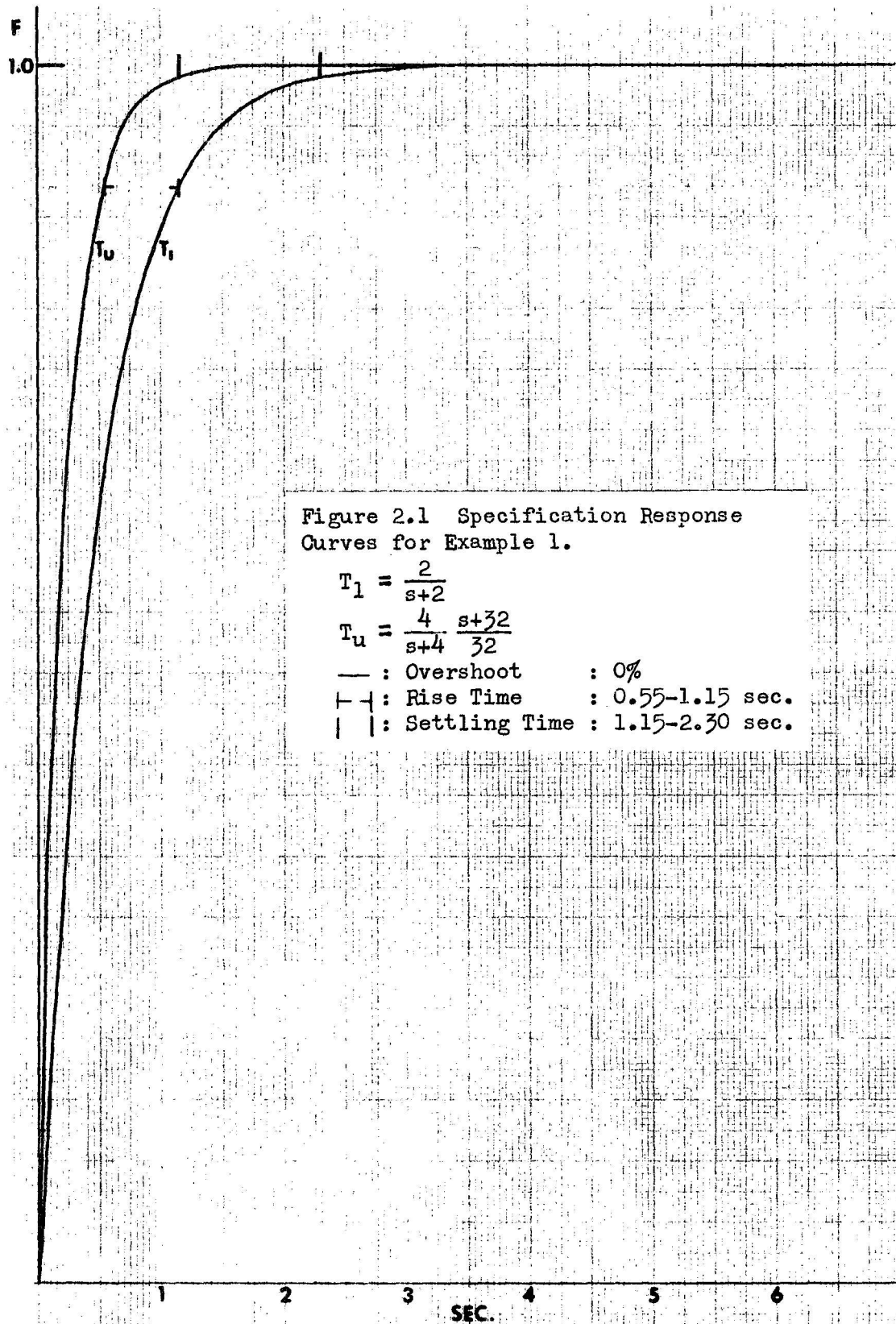
least one more than the excess poles over zeros of P_o ($e_P = 0$).

Similar considerations apply for other system configurations.

By reference to a "catalog of time response curves"* or by trial and error, find time response curves that just satisfy the given time domain specifications. In this example, the assumed first-order response was investigated to see if it would "fit" the given specification. It was found that the time response of the transfer function $T_1 = 2/(s+2)$ satisfies the requirements rise time = 1.15 seconds, settling time = 2.30 seconds, and 0% overshoot. See figure 2.1. If a first order response could not satisfy the time specifications, higher order transfer functions and/or pole-zero type transfer functions could be investigated.

In choosing T_U ($T(s)$ upper), it is desirable to pick a relaxed high frequency requirement (i.e., after a certain level is reached, e.g. -18 to -26 db, the magnitude remains constant) type transfer function. This gives a greater variation in $|T_m/T_U|$, which allows the $-L_O(j\omega)$ phase crossover to occur at a lower frequency than the excess pole type of transfer function (see step 2). In this example, the form $T_U = b(s+a)/a(s+b)$ was investigated to see if it's time response would "fit" the given specifications. It was found that the time response of the transfer function $T_U = 4(s+32)/32(s+4)$ satisfies the requirements rise time = 0.55 seconds, settling time = 1.15 seconds, and 0% overshoot. See figure 2.1.

*If this method of design is to be used for a large series of design problems with different desired specifications, it would be helpful to develop or maintain a catalog of time responses for incremental changes in a single parameter of a transfer function. For example, see {/}.



If an analog computer is available, the investigation of transfer functions to see if their time response fits the time specifications can be simplified by using Beck's method {8} to mechanize the transfer function.

Plot T_l and T_u on Bode plot. See figure 2.2.

Step 2) Select a "model" transfer function, T_m , whose Bode plot lies between those of T_l and T_u . Within these boundaries, the choice is pretty much arbitrary at this point. If it is later found that a conflict exist, then location of T_m can be shifted and/or the model and boundary transfer functions could be re-selected (see step 2, example 2, section 3.2). The problem seems to be partly in the matching of the "model" response to the response of the nominal plant. If, for example, the model is chosen such that its response is the minimum allowable and the nominal plant is chosen such that its response is the maximum possible, then, a change in plant parameter, (which must be a decrease in plant response) must cause an increase in system response in order for the system response to stay within specification. That is, the directions of change in plant response and system response are contrary. If this is the situation, then it can be expected that some difficulties (if not impossibilities) will be encountered in trying to form a $L_o(s)$ that follows the minimum boundaries on the complex plane specified by the particular choice of T_m and P_o . For this example the model transfer function was chosen equal to the lower boundary transfer function, i.e., $T_m = T_l = 2/(s+2)$, as this satisfies the above consideration and simplifies the calculations (see table 2.1, $|T_m/T_l|$ column). This was plotted on

figure 2.2 and the following calculations made;

If magnitude of T_m $\dot{=} x_m$, $20 \log x_m \dot{=} y_m$ db

and magnitude of T_i $\dot{=} x_i$, $20 \log x_i \dot{=} y_i$ db

then $20 \log x_m - 20 \log x_i = 20 \log (x_m/x_i)$

$$= (y_m - y_i) \text{ db}$$

or $\log (x_m/x_i) = [(y_m - y_i)/20] \text{ db}$

and $x_m/x_i = |T_m/T_i|$

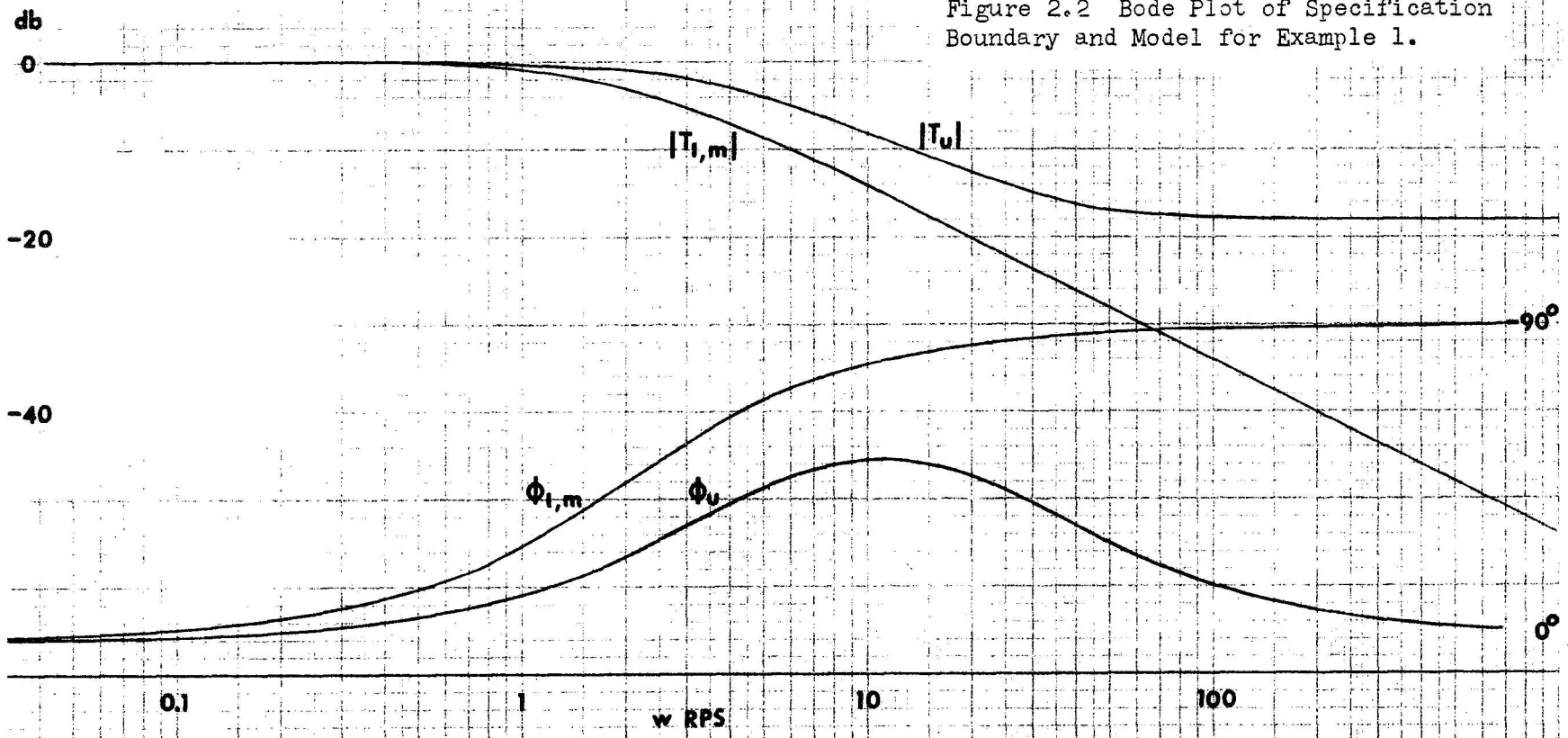
$$= \text{antilog of } [(y_m - y_i)/20] \text{ db}$$

therefore at:

$j\omega_x$ rps	$\angle T_m/T_u$	antilog of	$ T_m/T_u $	\leq	$ T_m/T $	\leq	$ T_m/T_1 $	= antilog of	$\angle T_m/T_1$
j0.8	-13°	-.0237db	0.947	"	1.0	0 db	0°		
j1.0	-15°	-.0353db	0.922	"	1.0	0 db	0°		
j2.0	-23°	-.100 db	0.794	"	1.0	0 db	0°		
j4.0	-25°	-.195 db	0.638	"	1.0	0 db	0°		
j8.0	-26°	-.255 db	0.556	"	1.0	0 db	0°		
j20	-38°	-.3495db	0.447	"	1.0	0 db	0°		
j40	-51°	-.510 db	0.309	"	1.0	0 db	0°		
j80	-68°	-.740 db	0.182	"	1.0	0 db	0°		
j200		-1.125db	0.075	"	1.0	0 db			

Table 2.1 Magnitude and Phase Ratios
for Example 1

For high frequencies the $-L_0$ minimum boundaries due to T_u (left side) must eventually lie in the 1st quadrant so that the $L_0(s)$ to be formed can cross the 180° phase line (positive real axis due to negative sign before L_0). Therefore, the selected ω_x 's should



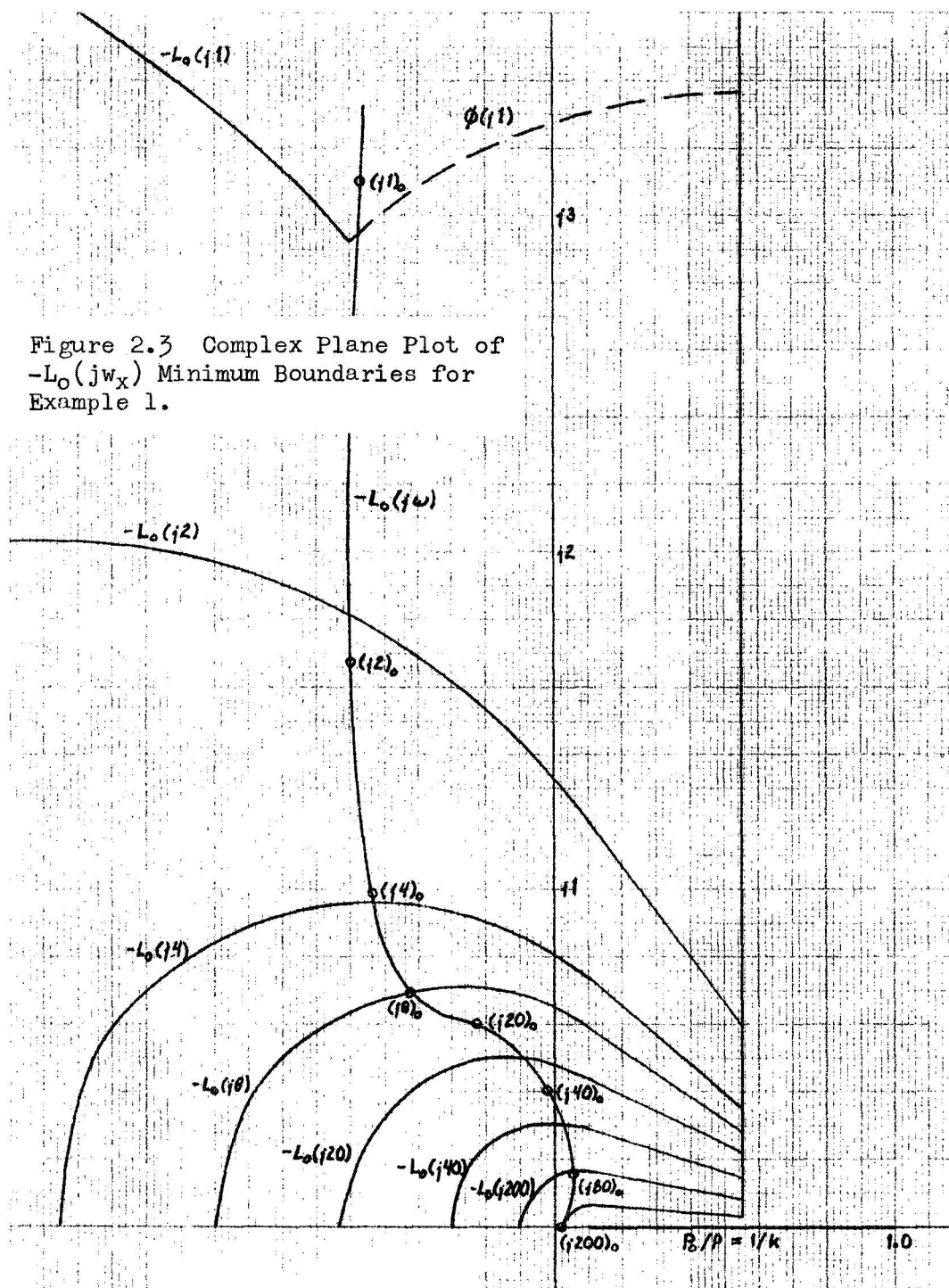
eventually be large enough to have this condition. See $jw_x = j100$ minimum boundary in figure 2.3.

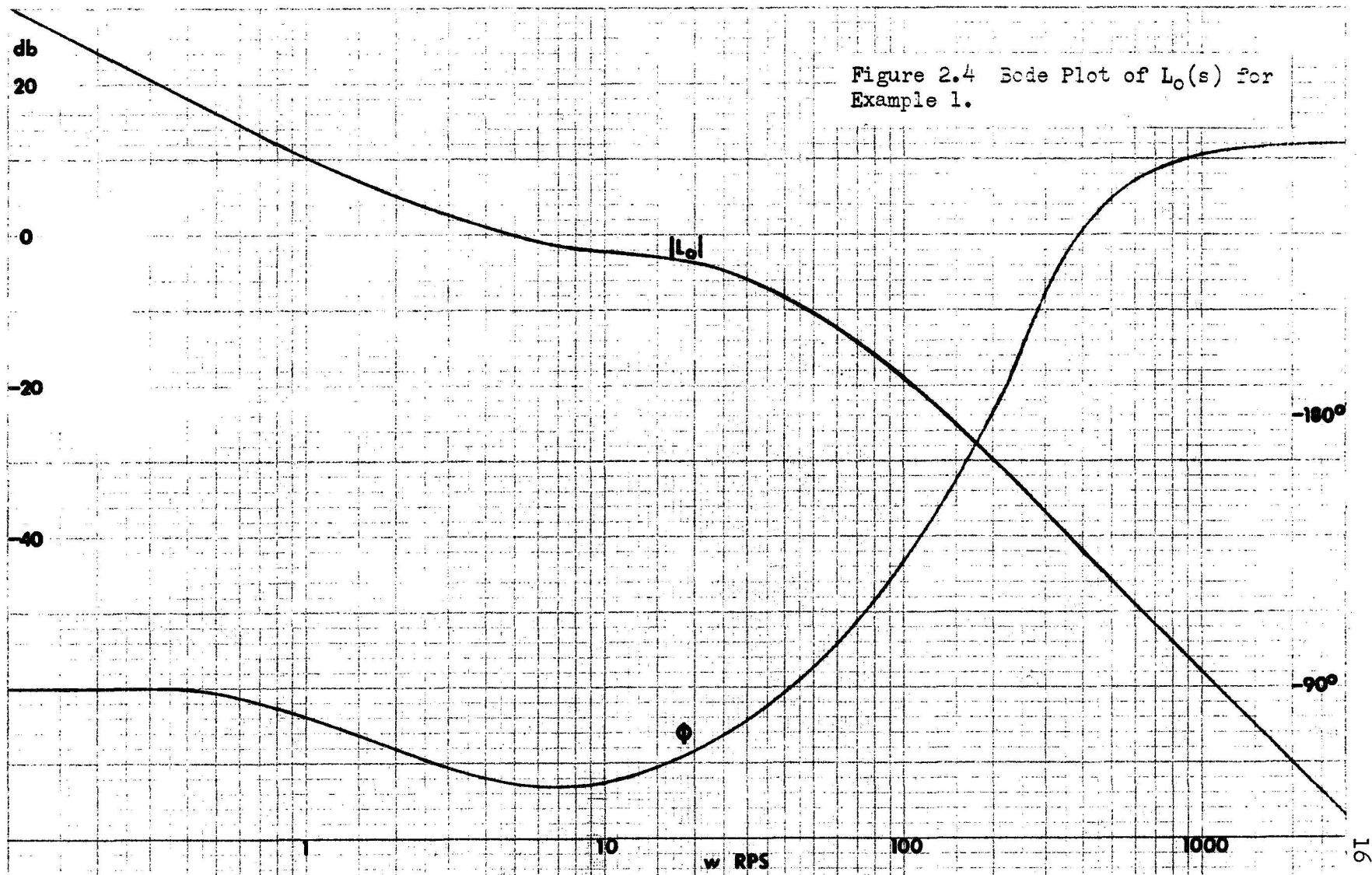
The excess pole type transfer function $T_u^i = 4.1/(s+4.1)$ approximately satisfies the upper specifications. If it was used (instead of $T_u = 4(s+32)/32(s+4)$) the ratio $|T_m/T_u^i|$ would be approximately 0.5 ($y_m - y_u \cong -6\text{db}$) for all $w \geq 15$ rps, and it would take a much larger bandwidth to reach the phase crossover of $L_o(jw)$. See discussion of step 1.

Step 3) Pick some value of the plant, within it's area of variation, to be the nominal value, $P_o(s)$. Usually it is that combination of plant parameter values which corresponds to minimum P {9}. Then $P_o/P \leq 1.0$, which facilitates the complex plane graphical procedure. However, if this particular choice of P_o (and T_m , see step 2) later leads to difficult or impossible conditions on $L_o(jw)$, it will be necessary to change the P_o, T_m combination by either re-selecting P_o or T_m or both. In this example $P_o = 1.0$ was picked. Then $0.1 \leq P_o/P \leq 1.0$ for all w 's. Resulting plot is shown on figure 2.3, and resulting $L_o(jw)$ on figure 2.4.

Step 4) Determining loci of $-L_o(jw_x)$ minimum boundaries. See reference {1} for details.

See figure 2.3. Observe that loci of $-L_o(jw_x)$ due to T_u (left side) must lie in 2nd and/or 1st quadrants of complex plane for low frequencies. Sometimes a particular choice of T_m will cause the $-L_o$ minimum boundary to lie in the 3rd quadrant, which implies a phase lead at low frequencies and hence possible difficulties (see step 2, section 3.2).





If this is the case, it is necessary to re-select T_m and repeat step 2 (see discussion of steps 2 and 3).

Step 5) Determining a feasible $L_o(j\omega)$ function. See reference {1} for details.

Note that in order to have zero steady-state error it is necessary to have a pole at $s = 0$, which means $-L_o$ must be asymptotic with the positive $j\omega$ axis (-90° , since phase lag measured in clockwise direction from negative real axis) for very low frequencies. See figures 2.3 and 2.4.

For this example, $L_o(s) = (3.2)(27)(60)(s+4)/4s(s+27)(s+60)$ was chosen.

Step 6) If desired system configuration is two-degree-of-freedom system shown in figure 2.5, then,

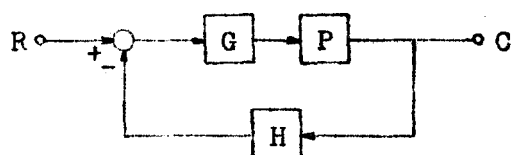


Figure 2.5 Two-degree-of-freedom system.

$$T = C/R = GP/(1+L) \quad (1)$$

$$\text{where } L = GPH, \quad (2)$$

P is the plant transfer function, and G and H are compensation blocks

available to the designer. Now if $P = P_o$ (some nominal value of P), then (1) and (2) becomes

$$GP_o/(1+L_o) \approx T_o \equiv T_m \quad \text{or} \quad G = \frac{T_m}{P_o} (1+L_o) \quad (3)$$

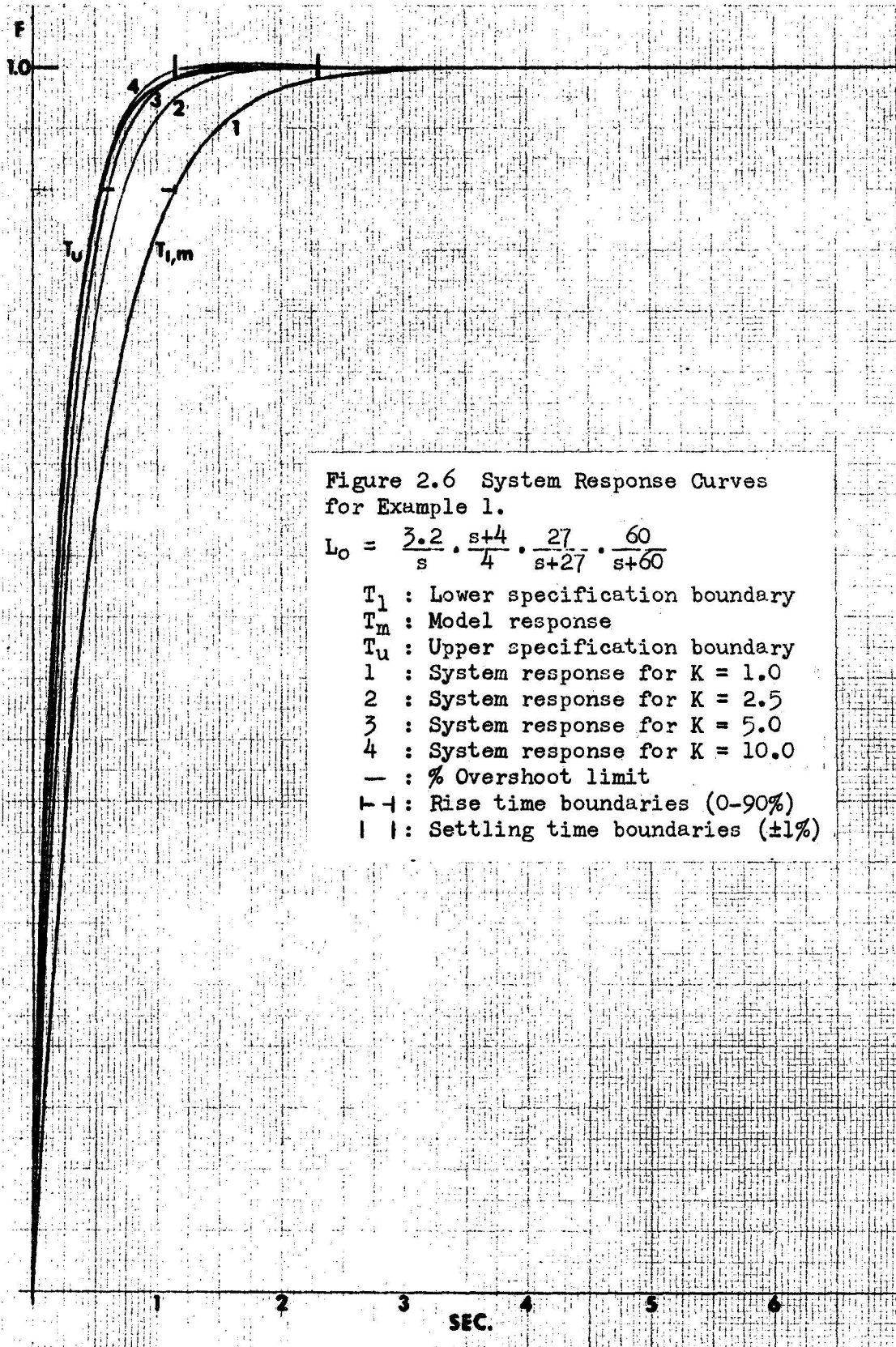
$$\text{and } GP_oH \approx L_o \quad \text{or} \quad H = \frac{L_o}{P_o G} = \frac{L_o}{T_m} \times \frac{1}{1+L_o} \quad (4)$$

Therefore $T = GP/(1+GPH)$

$$\begin{aligned}
 &= \frac{T_m(1+L_o)P/P_o}{1 + \frac{T_m}{P_o} (1+L_o) \cdot P \cdot \frac{L_o}{T_m(1+L_o)}} = \frac{T_m(1+L_o)P}{P_o + PL_o} \\
 &= \frac{2}{s+2} \cdot \frac{s^3 + 87s^2 + 2916s + 5184}{s^3 + 87s^2 + 1620s} k \\
 &= \frac{1 + 1296k(s+4)/(s^3 + 87s^2 + 1620s)}{s+2} \\
 &= \frac{2}{s+2} \cdot \frac{k(s^3 + 87s^2 + 2916s + 5184)}{(s^3 + 87s^2 + 1620s) + 1296k(s+4)}
 \end{aligned}$$

2.2 Analysis

The system time response results are shown on figure 2.6. For $k = 5$ and 10 (curves 3 and 4), there is a slight amount of overshoot (0.34% for $k = 10$), however it is within the settling time limits ($\pm 1\%$) and, hence, was considered within specification. With the above slight exception, the design procedure seems to work exceedingly well, at least for the simple system chosen. The available time domain specification space (boundaries shown as T_l and T_u in figure 2.6) is completely used and the response is of the nature specified by T_m . Because the specification space is totally used, it is suspected that the design approaches an optimum in terms of being most economical in gain and bandwidth requirements. In the later multiple case examples (examples 3 and 4), these points will be discussed in more detail.



CHAPTER 111

SECOND-ORDER MODEL

3.1 Purpose of Second-order Model

In chapter 2, a simple first-order model was investigated to see if the "modeling" technique would work. For that purpose, a simple gain changing plant was assumed, and the results were very encouraging. In this chapter, a more complex and realistic second-order plant with varying gain, frequency, and damping factor is assumed. All plant parameters are permitted to vary in an arbitrary manner, within the limits specified. However, rate of variation is assumed to be slow when compared to system response time so that time dependence at the parameters is not a factor. A second-order model (first without overshoot, then with some overshoot allowed by the specification) will be investigated to see if a successful design can be accomplished.

3.2 Example 2, Second-order Model Without Overshoot

Given: Plant transfer-function $P(s) = kw_p^2 / (s^2 + 2z_p w_p s + w_p^2)$

with parameter variations: $1 \leq k \leq 10$

$$1 \leq w_p \leq 3$$

$$0.6 \geq z_p \geq 0.2$$

and desired time domain specifications as follows:

Rise time, 0 to 90% : 1.15 to 3.95 seconds

Settling time, $\pm 1\%$: 2.25 to 7.50 seconds

Overshoot limit : 0%

Step 1) Finding time specification boundaries.

The desired system configuration is to be the verification model two-degree-of-freedom system (see section 1.6), hence, T_1 and L_0

must only have an excess of poles over zeros (see step 1, example 1, section 2.1). Therefore, assuming a second-order model a second-order T_1 is permissible.

By trial and error, it was found that the time response of the transfer function $T_1 = 1/(s+1)^2$ satisfies the requirements rise time = 3.95 seconds, settling time = 7.50 seconds, and 0% overshoot. Similarly it was found that the time response of transfer function $T_u = 9(s+12)^2/144(s+3)^2$ satisfies the requirements rise time = 1.15 seconds, settling time = 2.25 seconds, and 0% overshoot. See figure 3.2.

Step 2) Initially T_m was chosen equal to T_1 to simplify calculations as in example 1. However, for the P_o chosen (see step 3) this caused the $-L_o(jw_x)$ loci, for $jw_x = j0.4$ rps, and lower frequencies, to lie in the third quadrant of the complex plane. See figure 3.1, for $jw_x = j0.4$.

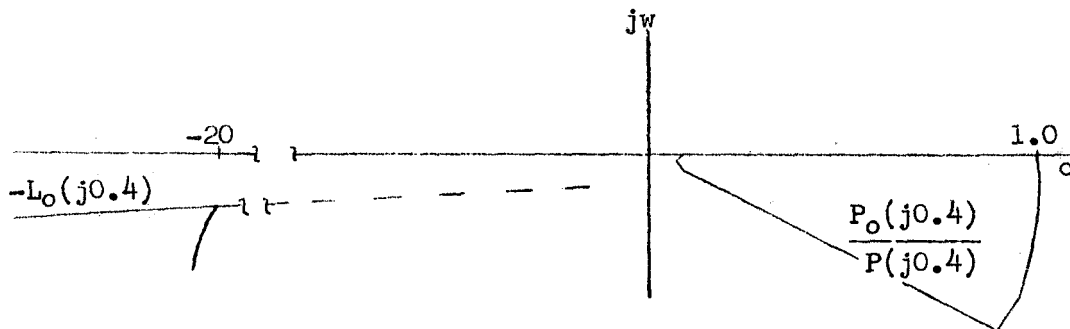


Figure 3.1 Example of Phase Lead.

This would require $L_o(s)$ to have a phase lead of about 100° 's or more (since L_o is to have a pole at the origin) which might be

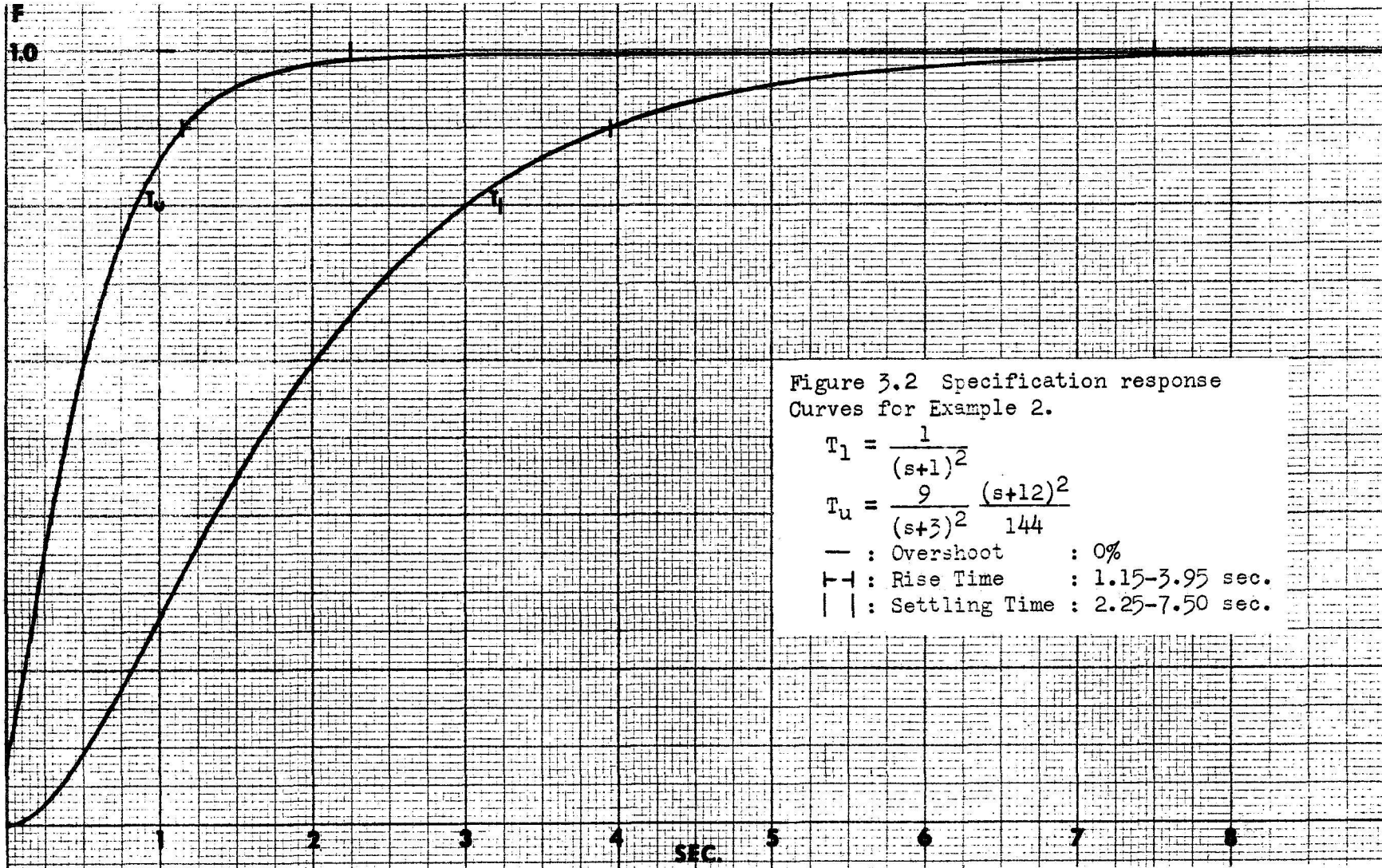


Figure 3.2 Specification response Curves for Example 2.

$$T_l = \frac{1}{(s+1)^2}$$

$$T_u = \frac{9}{(s+3)^2} \frac{(s+12)^2}{144}$$

- : Overshoot : 0%
- ↑ : Rise Time : 1.15-3.95 sec.
- || : Settling Time : 2.25-7.50 sec.

difficult to realize. At this point it is necessary to change T_m or P_o . It was decided to change T_m to the middle of the allowable area between T_l and T_u , i.e. $T_m = 4/(s+2)^2$. See figure 3.3. The $-L_o(jw_x)$ loci for low frequencies then lies in the second quadrant as desired. See figure 3.4. The following calculation were made from Bode plot, figure 3.3 (see step 2, example 1, section 2.1 for method).

$\angle T_m/T_u$	$ T_m/T_u $	w_x rps	$ T_m/T_l $	$\angle T_m/T_l$
-11.28°	.955	0.4	1.109	20.96°
-21.36°	.891	0.8	1.396	33.60°
-25.80°	.861	1.0	1.567	36.81°
-41.54°	.708	2.0	2.512	36.86°
-57.46°	.501	4.0	3.388	24.44°
-78.80°	.309	8.0	3.802	14.45°
-90.38°	.2455	10.0	3.890	11.16°
-123.75°	.1035	20.0	3.890	5.74°
-143.46°	.0343	40.0	3.981	2.86°
-164.29°	.00933	80.0	3.981	1.44°
-167.96°	.00625	100.0	3.981	1.14°
-173.70°	.00524	200.0	3.981	.54°

Table 3.1 Magnitude and Phase Ratios
for Example 2.

Step 3) Again, as in step 3 of example 1 (section 2.1), the minimum value of $P(s)$ was picked to be nominal value, $P_o(s)$, i.e. $P_o(s) = 1/(s^2+1.2s+1)$. The required calculations were performed

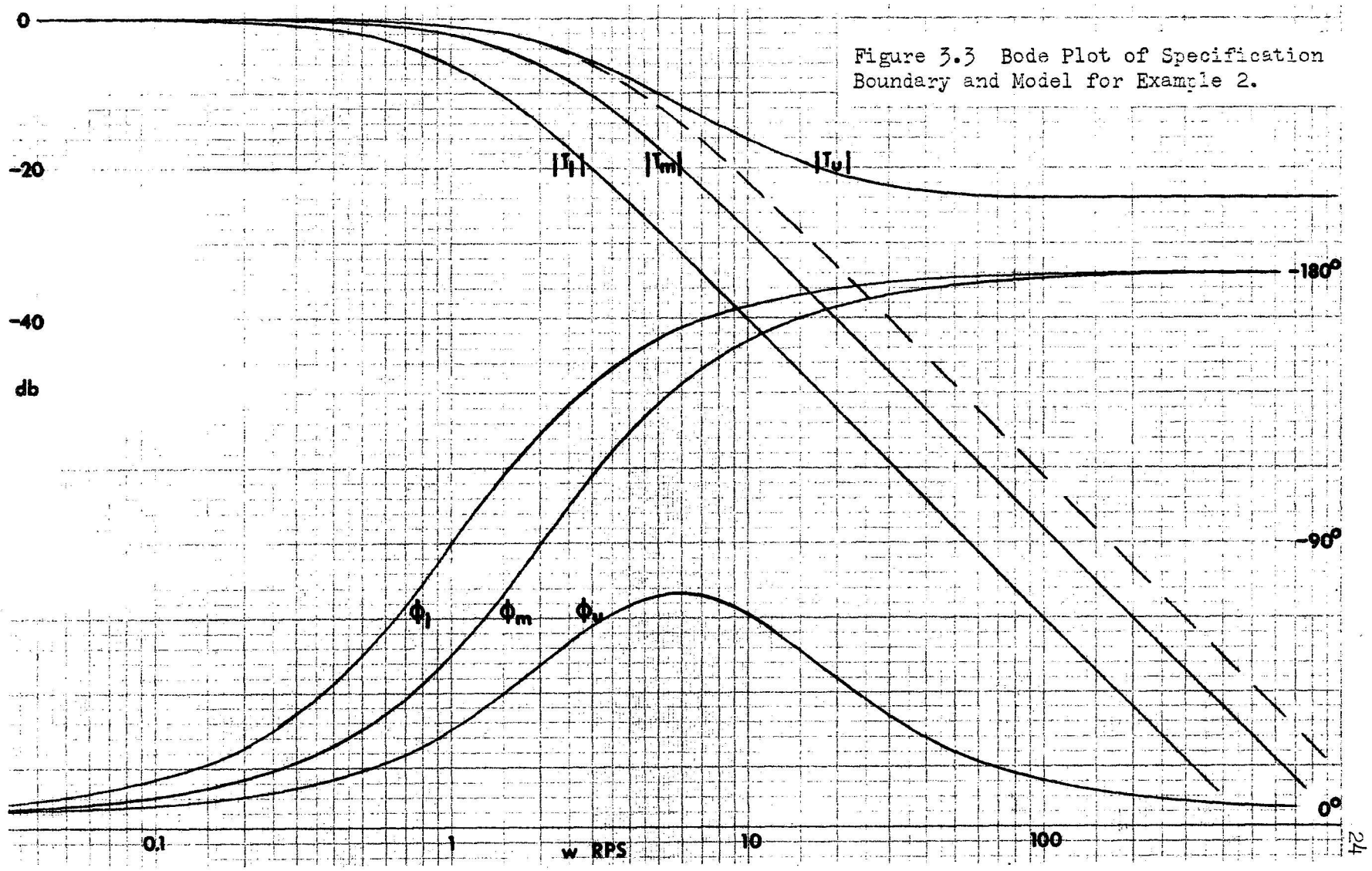


Figure 3.3 Bode Plot of Specification Boundary and Model for Example 2.

(see reference {1} for details and appendix A for table of $P_0(j\omega_x)/P(j\omega_x)$ data) and the results are shown on complex plane plot, figure 3.4.

Steps 4 and 5) Determining $-L_0(j\omega_x)$ minimum boundaries loci and feasible $L_0(j\omega)$ function as per design procedure given in reference {1}. For this example, $L_0(s) = (2.5)(25)/s(s+25)$ and is plotted in figure 3.5.

Step 6) System configuration is the verification model (see section 1.6), so that

$$\begin{aligned}
 T &= \frac{T_m(1+L_0)P}{P_0+PL_0} \\
 &= \frac{4}{(s+2)^2} \cdot \frac{s^2+25s+62.5}{s^2+25s} \cdot \frac{kw^2}{s^2+2z_p w_p s+w_p^2} \\
 &= \frac{1}{s^2+1.2s+1} + \frac{kw^2}{s^2+2z_p w_p s+w_p^2} \cdot \frac{62.5}{s^2+25s} \\
 &= \frac{4}{(s+2)^2} \cdot \frac{(s^2+25s+62.5) kw^2(s^2+1.2s+1)}{(s^2+25s)(s^2+2z_p w_p s+w_p^2) + 62.5kw^2(s^2+1.2s+1)}
 \end{aligned}$$

3.3 Analysis of Example 2, Second-order Model Without Overshoot

The system time response results are shown on figure 3.6. For $K = 1$, $w_p = 1$, $z_p = 0.2$ (curve 2 of figure 3.6), the system response has a slight undershoot (flattens out) which may be undesirable although still within specification. This is probably caused by the system poles, due to the plant, being too far away from the compensation zeros, $P_0(s)$ to provide effective cancellation, and the pole from the origin not moving out far enough (only reached $\sigma = 1.4$). See pole-zero plot of transfer function (for system response shown in figure 3.6), figure 3.7.

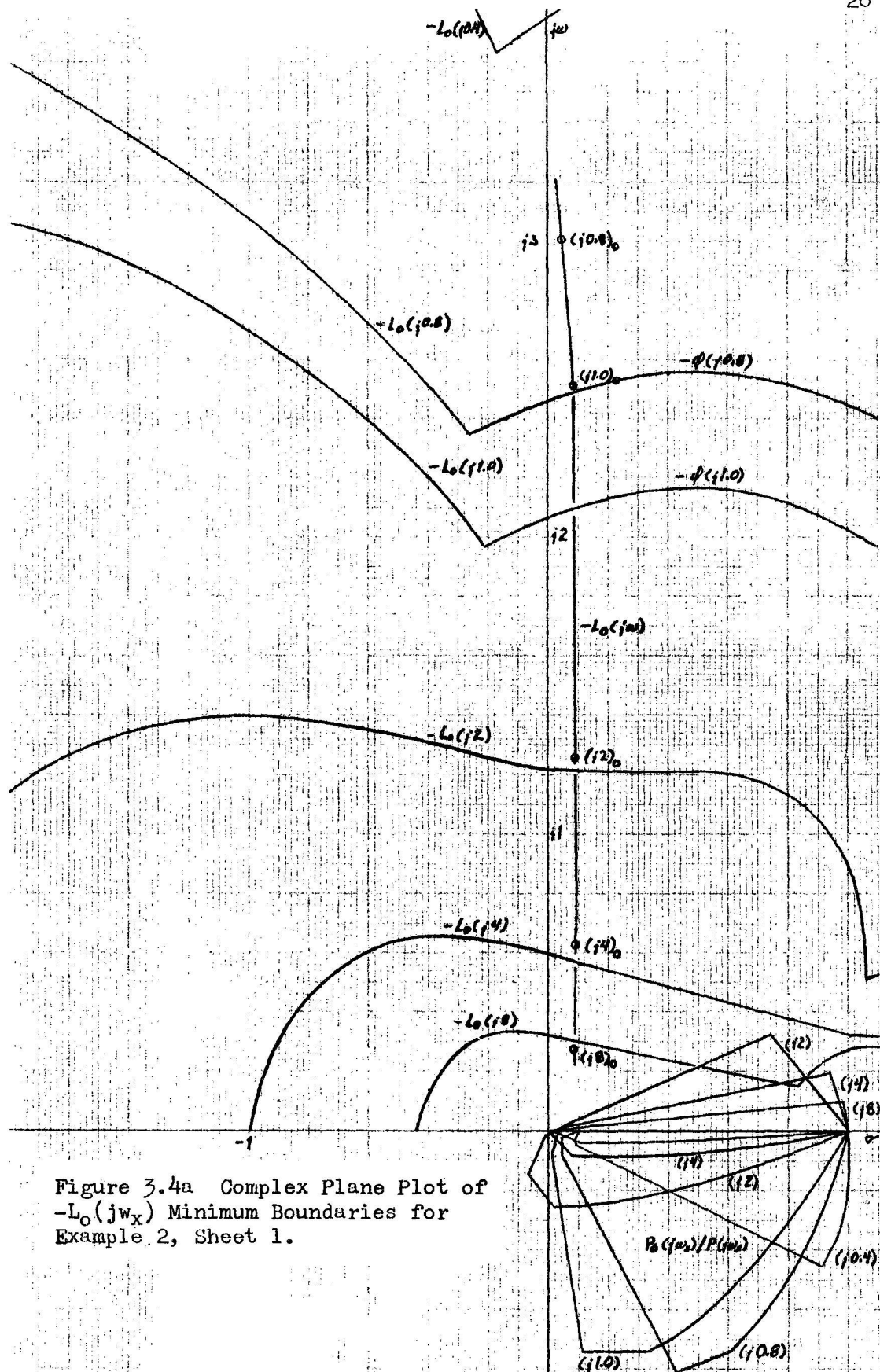
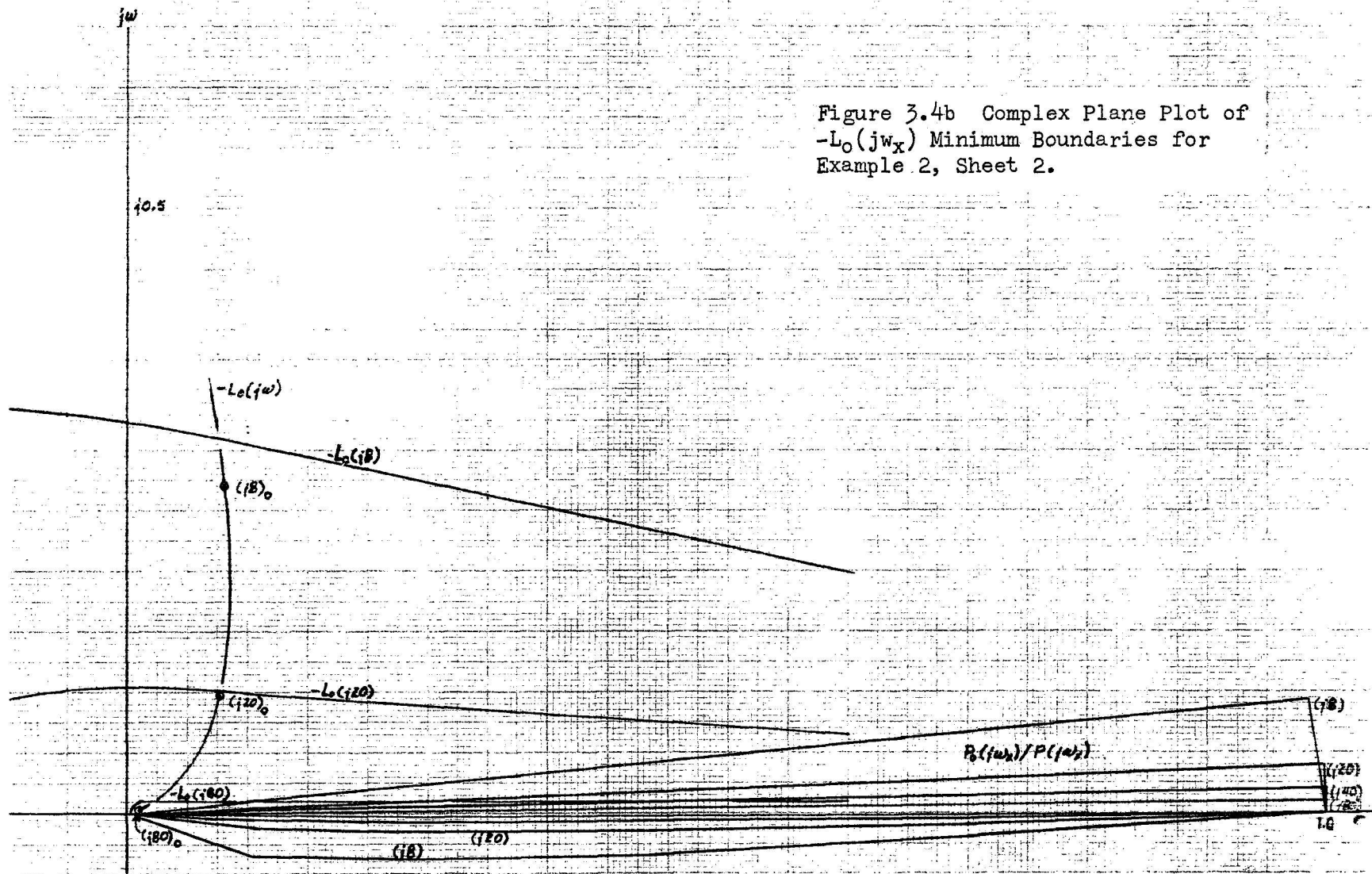


Figure 3.4a Complex Plane Plot of $-L_0(jw_x)$ Minimum Boundaries for Example 2, Sheet 1.

Figure 3.4b Complex Plane Plot of $-L_o(j\omega_x)$ Minimum Boundaries for Example 2, Sheet 2.



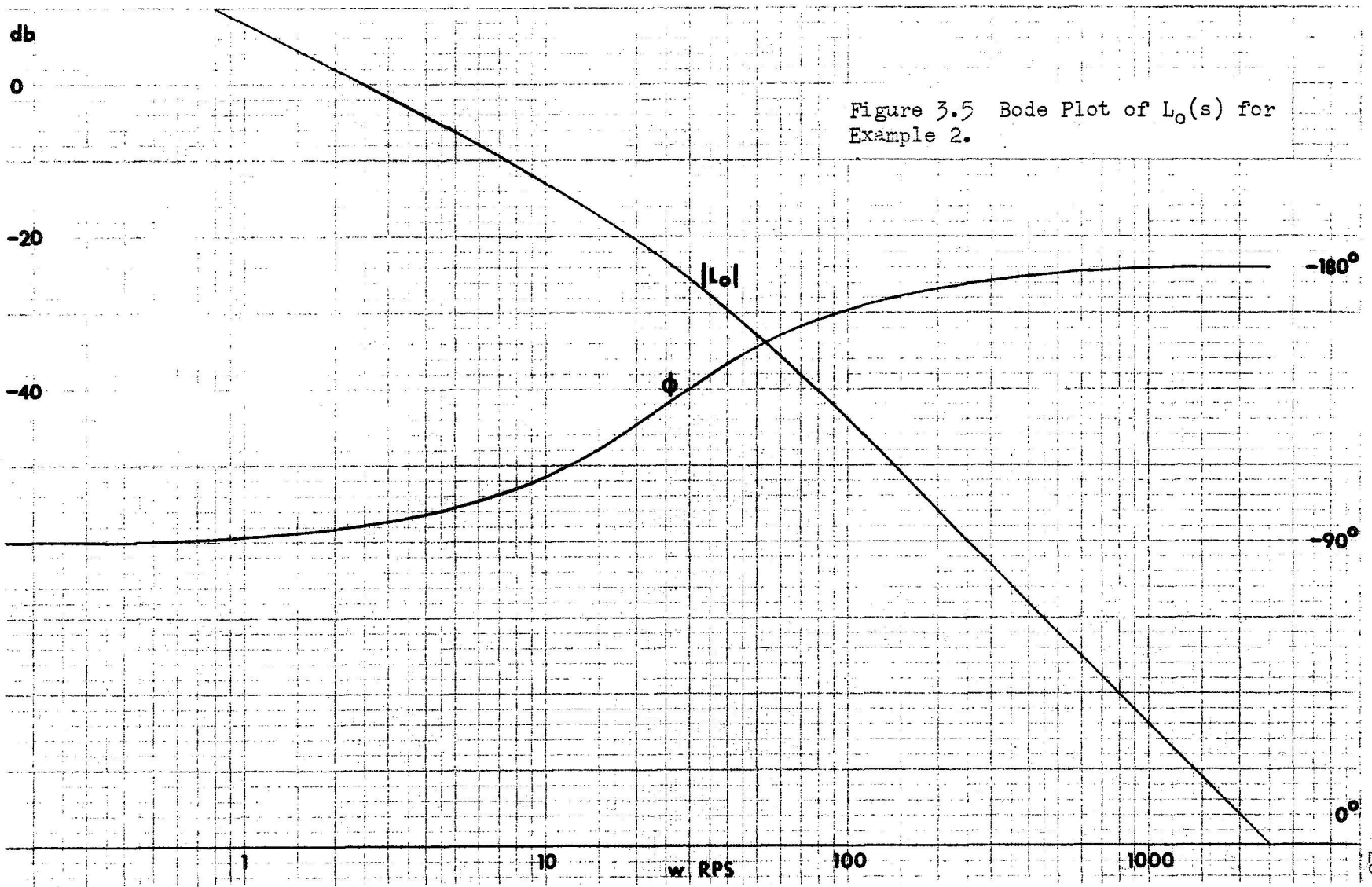


Figure 3.5 Bode Plot of $L_o(s)$ for Example 2.

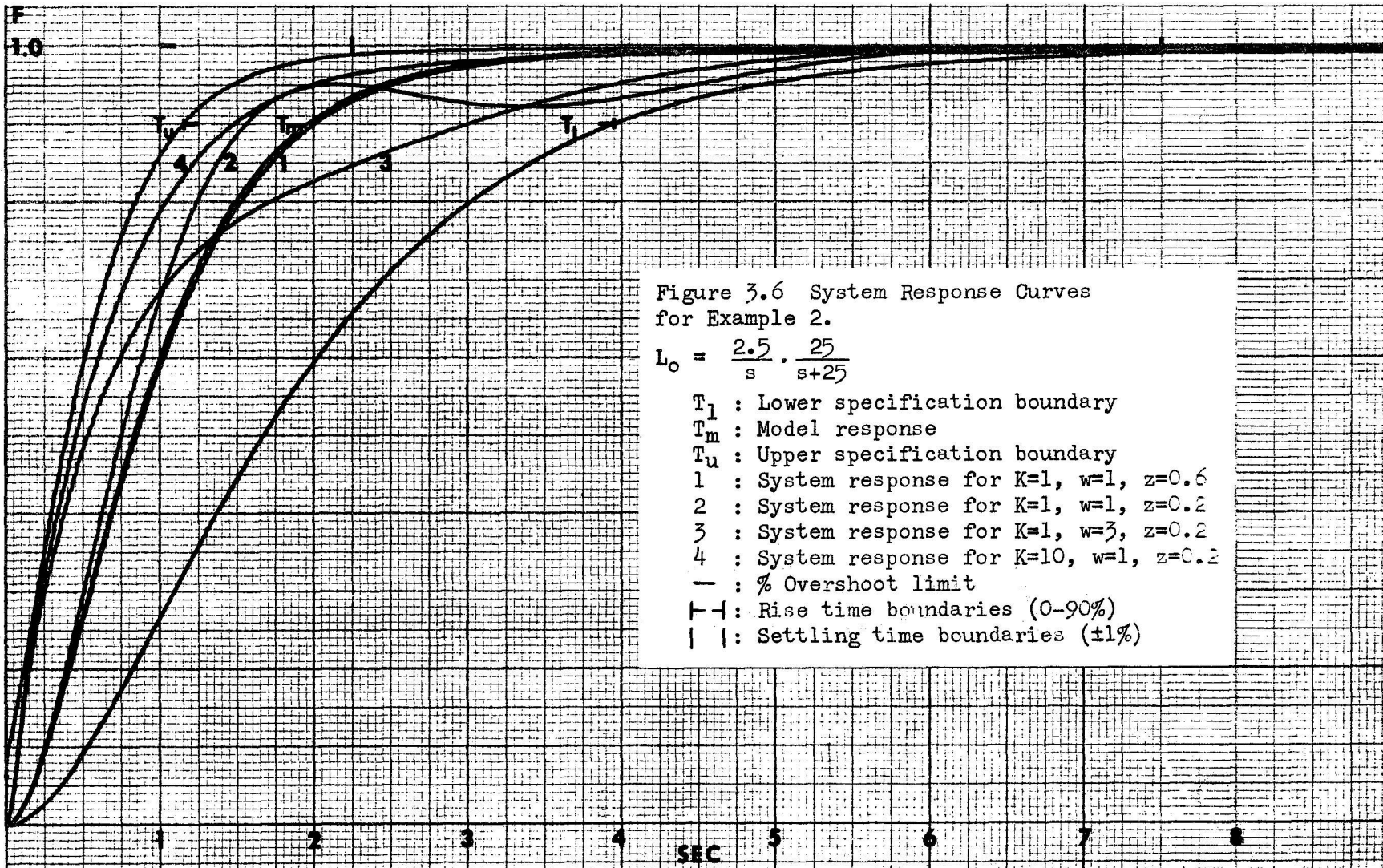


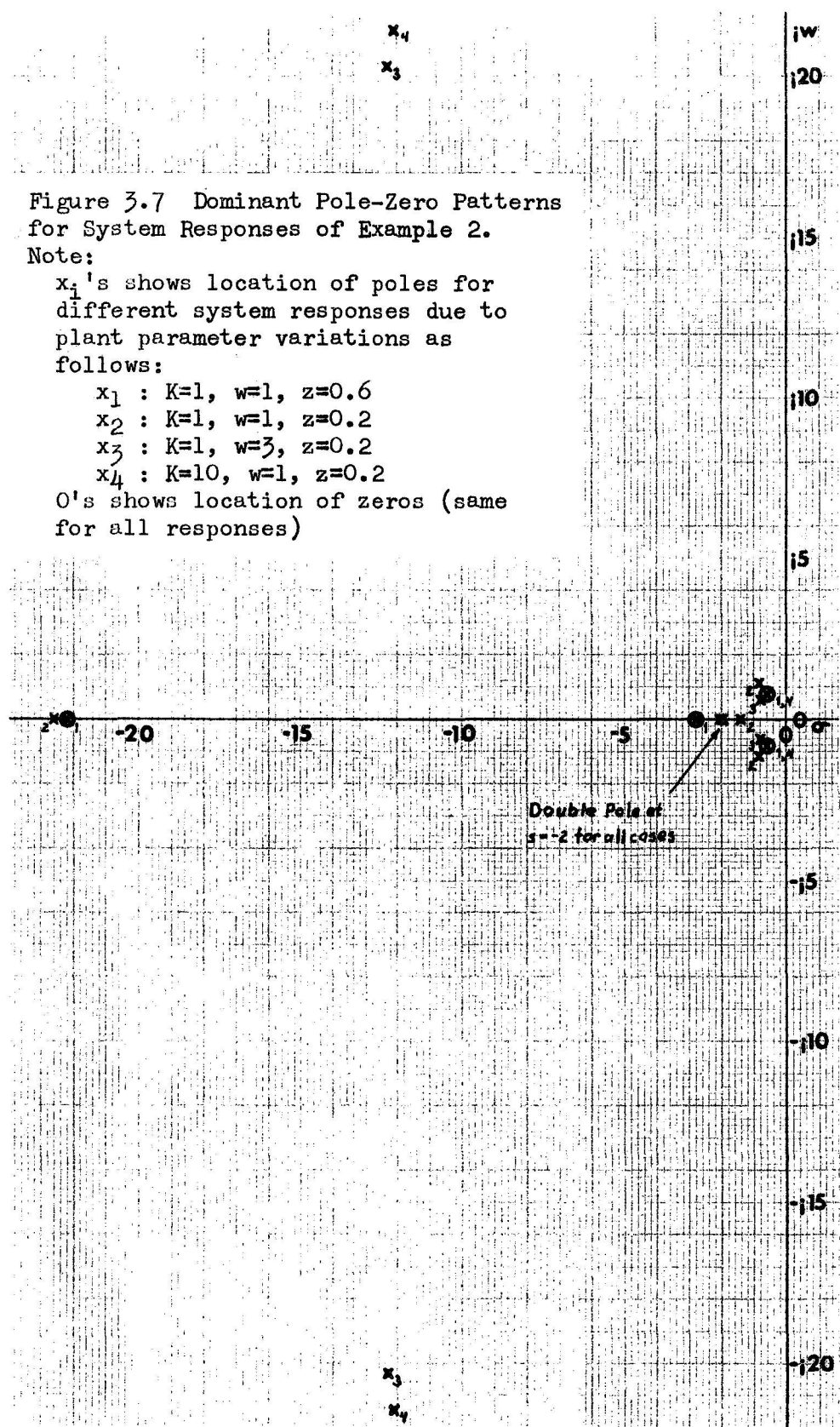
Figure 3.7 Dominant Pole-Zero Patterns for System Responses of Example 2.

Note:

x_i 's shows location of poles for different system responses due to plant parameter variations as follows:

- x_1 : $K=1, w=1, z=0.6$
- x_2 : $K=1, w=1, z=0.2$
- x_3 : $K=1, w=3, z=0.2$
- x_4 : $K=10, w=1, z=0.2$

0's shows location of zeros (same for all responses)



For $K = 1$, $P = P_0$, (response 1) actual cancellation occurs and the system response is that of the selected "model". For responses 3 and 4, the pole from the origin combines with a far-off pole and become a complex pair of far-off poles. If the undershoot is undesirable, then moving the compensation zeros ($P_0(s)$) toward the location of the complex poles for response 2 could be attempted. However, if undershoot restriction is not part of the specifications then the system response is within specification and the design is successful.

3.4 Example 3, Second-order Model With 10% Allowable Overshoot

Given: Plant transfer function, $P(s) = kw_p^2/(s^2+2z_pw_p s+w_p^2)$,

with parameter variations: $1 \leq k \leq 10$,

$$1 \leq w_p \leq 3,$$

$$0.6 \geq z_p \geq 0.2.$$

and desired time domain specifications as follows:

Rise time, 0 to 90% : 0.90 to 3.95 seconds,

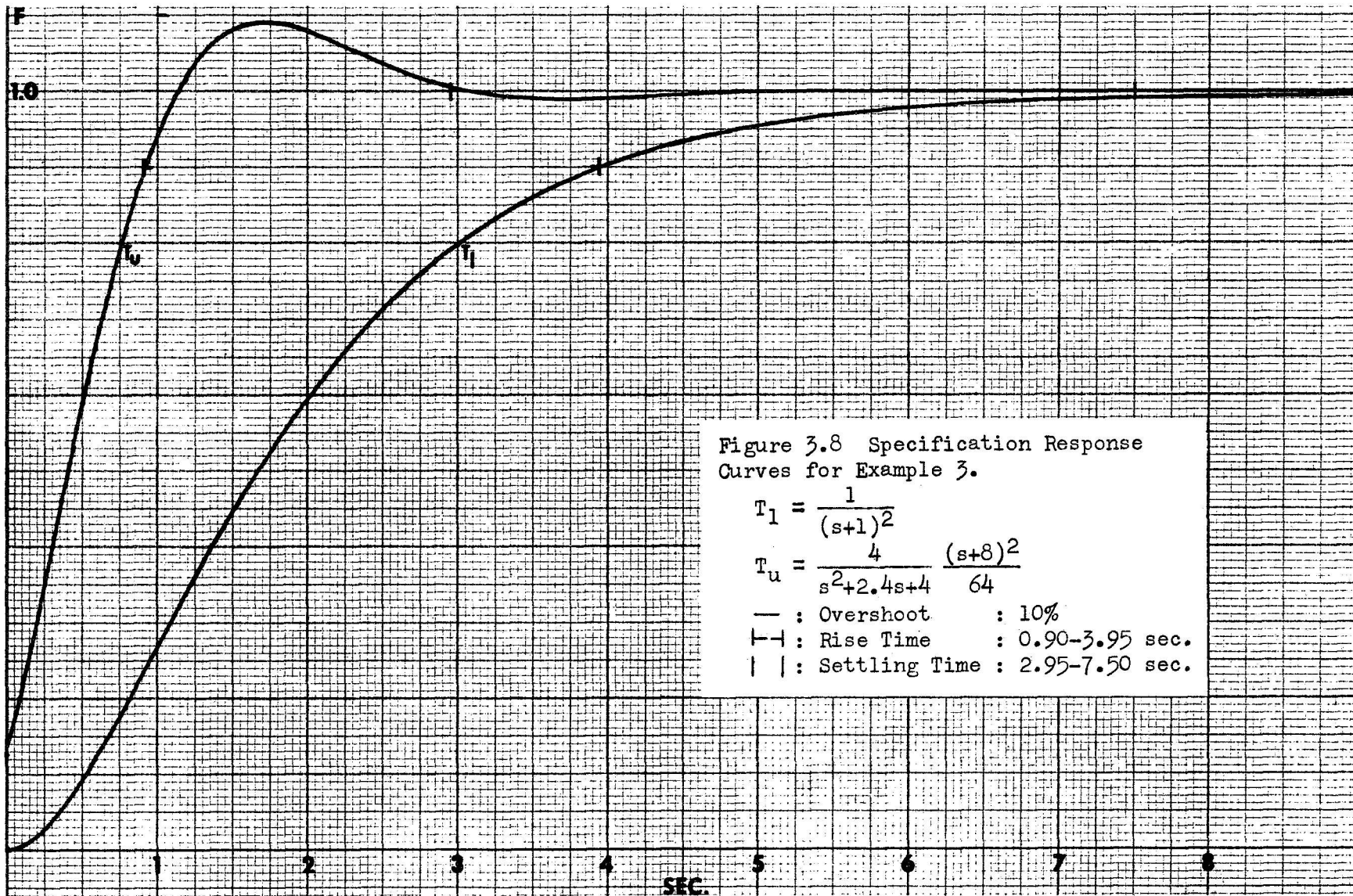
Settling time, $\pm 1\%$: 2.95 to 7.50 seconds.

Overshoot limit : 10%

Step 1) Finding time specification boundaries.

The desired system configuration will be the same as example 2 (section 3.2). Also, since the lower specifications are the same as example 2, the same $T_1 = 1/(s+1)^2$ is used for the lower boundary.

By investigating time responses of transfer functions of the nature $T_u = b(s+c)^2/c^2(s^2+as+b)$, it was found that $T_u = 4(s+8)^2/64(s^2+2.4s+4)$ approximately satisfies the requirements rise time = 0.90 seconds and settling time = 2.95 seconds with 10% overshoot. See figure 3.8.



Step 2) Choosing T_m . The same T_m as example 2 (step 2, section 3.2) was chosen, $T_m = 4/(s+2)^2$, as it still lies approximately in middle of area between T_1 and T_u of this example. See figure 3.9. The following calculations were then made from figure 3.9.

$\angle T_m/T_u$	$ T_m/T_u $	w_x rps	$ T_m/T_1 $	$\angle T_m/T_1$
-14.33°	.933	0.4	1.101	20.96°
-25.28°	.793	0.8	1.396	33.6°
-28.72°	.7245	1.0	1.567	36.81°
-30.47°	.543	2.0	2.512	36.86°
-36.65°	.596	4.0	3.388	24.44°
-79.04°	.462	8.0	3.802	14.45°
-93.90°	.380	10.0	3.890	11.16°
-133.29°	.129	20.0	3.890	5.74°
-155.10°	.0359	40.0	3.981	2.86°
-167.41°	.00933	80.0	3.981	1.44°

Table 3.2 Magnitude and Phase Ratios
for Example 3.

Step 3) Choosing $P_o(s)$. The same P_o used in example 2 (step 3, section 3.2) was chosen. See reference {1} for details of method, appendix A for $P_o(jw_x)/P(jw_x)$ data, and figure 3.10 for resulting plot.

Steps 4 and 5) Determining loci of $-L_o(jw_x)$ minimum boundaries and feasible $L_o(jw)$ function. See design details given in reference {1}.

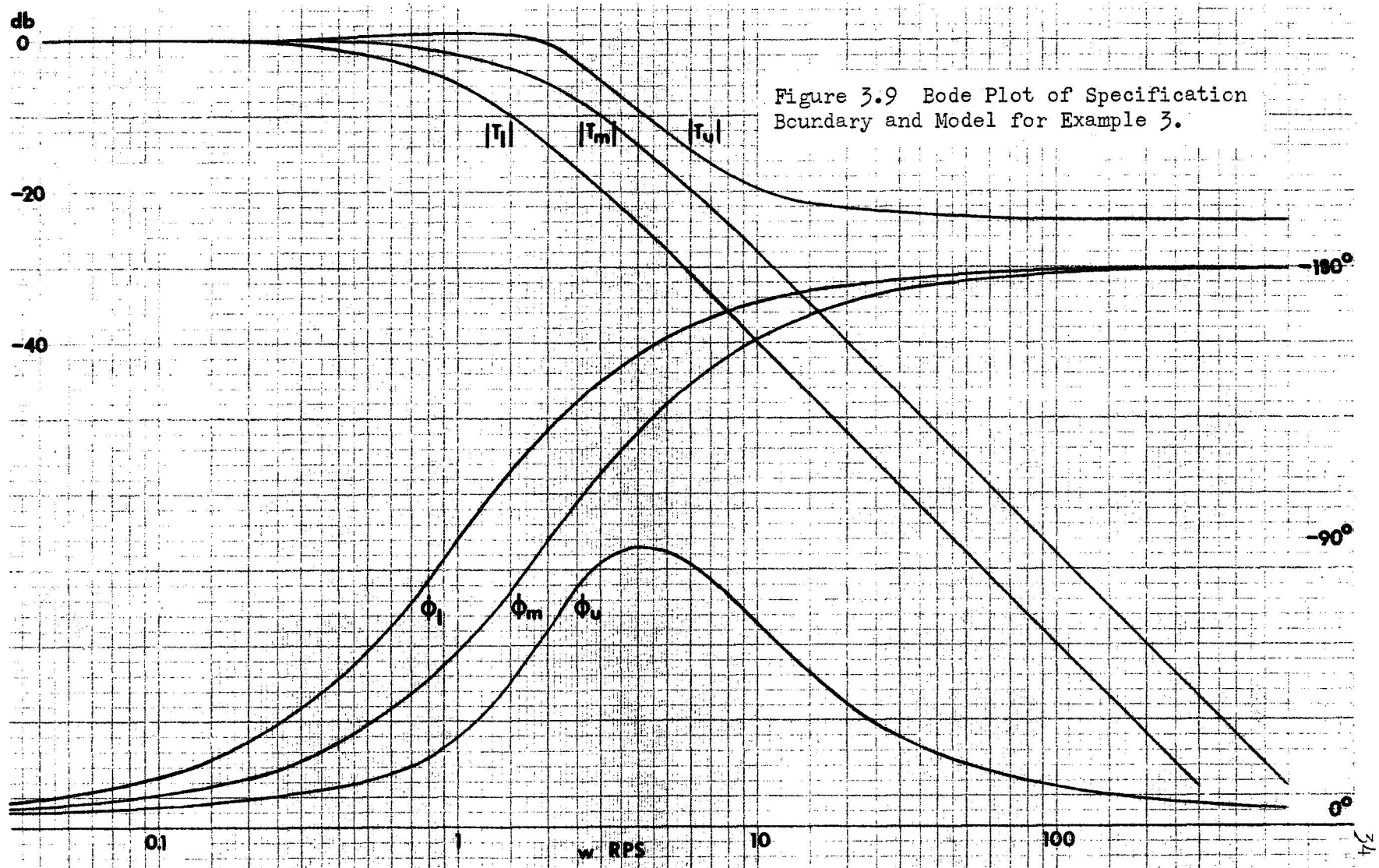


Figure 3.9 Bode Plot of Specification Boundary and Model for Example 3.

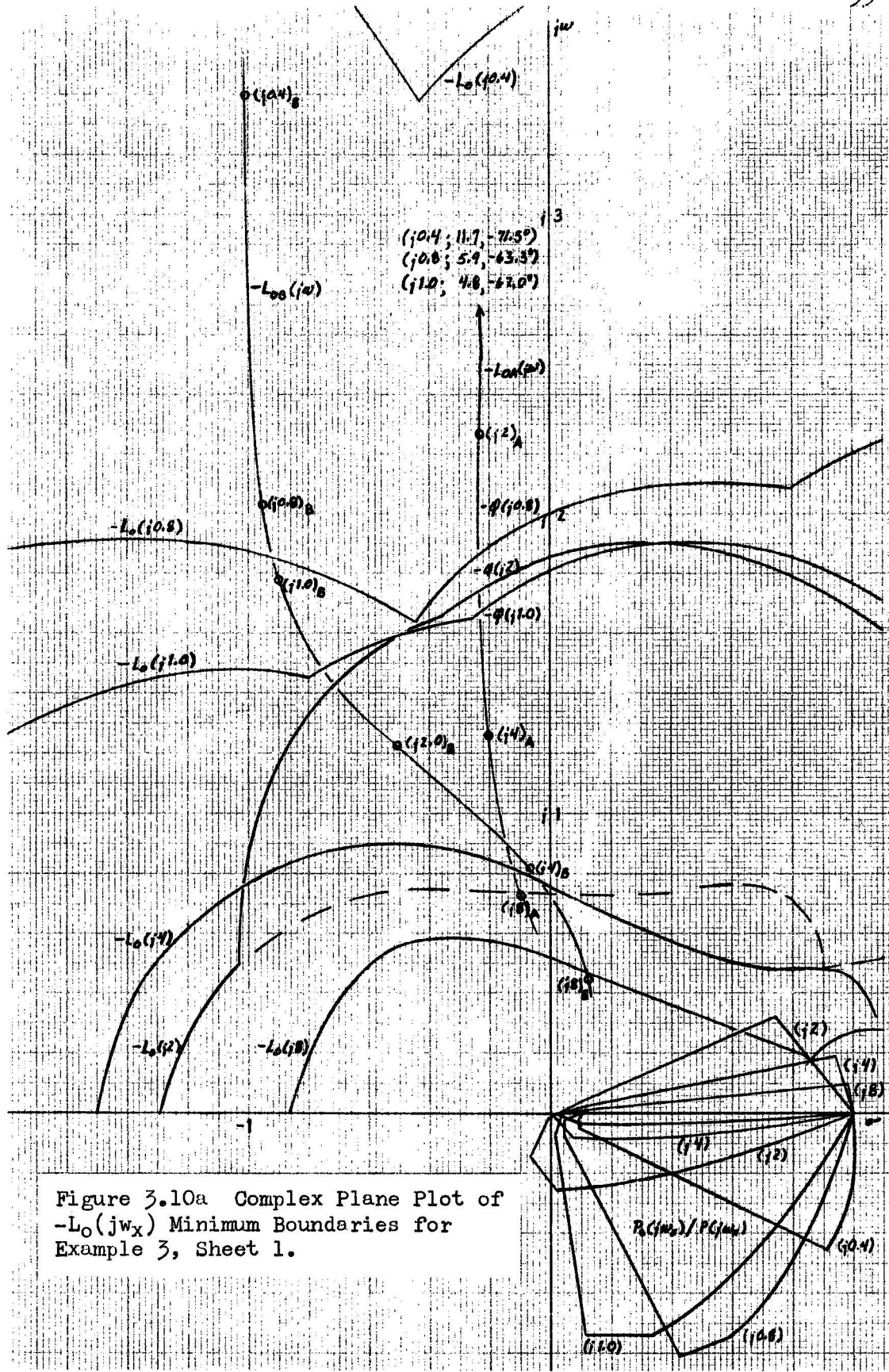


Figure 3.10a Complex Plane Plot of $-L_0(j\omega_x)$ Minimum Boundaries for Example 3, Sheet 1.

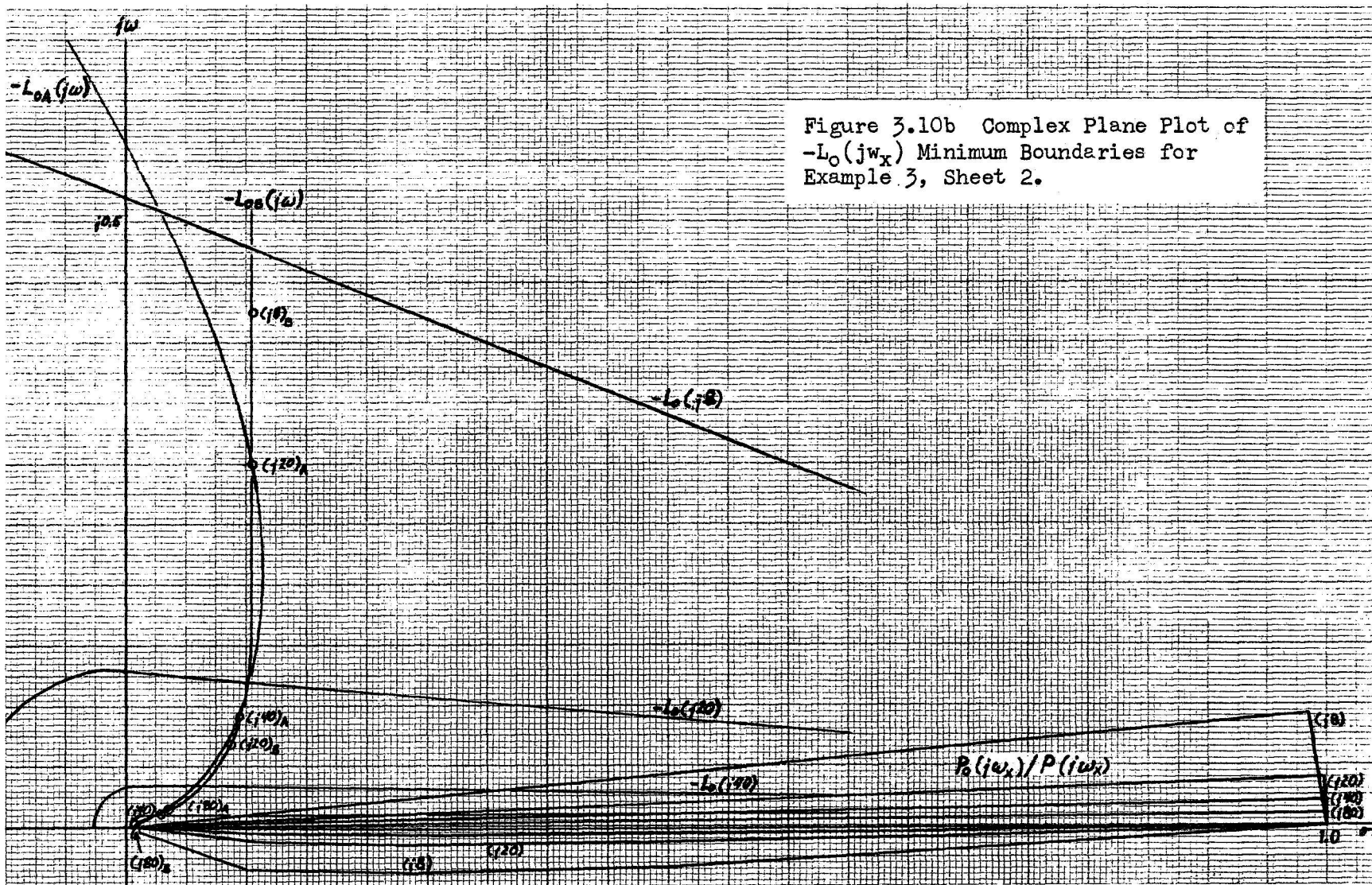


Figure 3.10b Complex Plane Plot of $-L_0(j\omega_x)$ Minimum Boundaries for Example 3, Sheet 2.

For this example, two different L_o 's were formed,

$$L_{oA} = (4.4)(20^2)(s+7)/7s(s+20)^2 \text{ and,}$$

$$L_{oB} = (1.2^2)(2.7)(12.5)(s+0.8)/0.8s(s+2.7)(s+12.5).$$

See figure 3.11.

The first, L_{oA} , was an initial attempt. The second, L_{oB} , was a result of trying to form a better design and use more of the allowable specification space.

Step 6) System configuration is the verification model (see section 1.6), so that

$$T = \frac{T_m(1+L_o)P}{P_o+PL_o}$$

$$\text{or } T_A = T_m [(s^3+40s^2+651.43s+1760) kw^2(s^2+1.2s+1)] + \\ [(s^3+40s^2+400s)(s^2+2z_p w_p s+w_p^2) + \\ 251.43kw^2(s+7)(s^2+1.2s+1)]$$

$$\text{and } T_B = T_m [(s^3+15.2s^2+86.48s+42.19) kw^2(s^2+1.2s+1)] + \\ [(s^3+15.2s^2+33.75s)(s^2+2z_p w_p s+w_p^2) + \\ 52.73kw^2(s+0.8)(s^2+1.2s+1)]$$

$$\text{where } T_m = 4/(s+2)^2$$

3.5 Analysis of Example 3, Second-order Model With 10% Allowable Overshoot

The system time response results are shown on figure 3.12 a & b. Observe that in case A, figure 3.12a, the response curves are closely grouped together and does not effectively utilize the allowable specification space. Referring to the complex plane, figure 3.10, it can be seen that L_{oA} is conservative in that the actual location

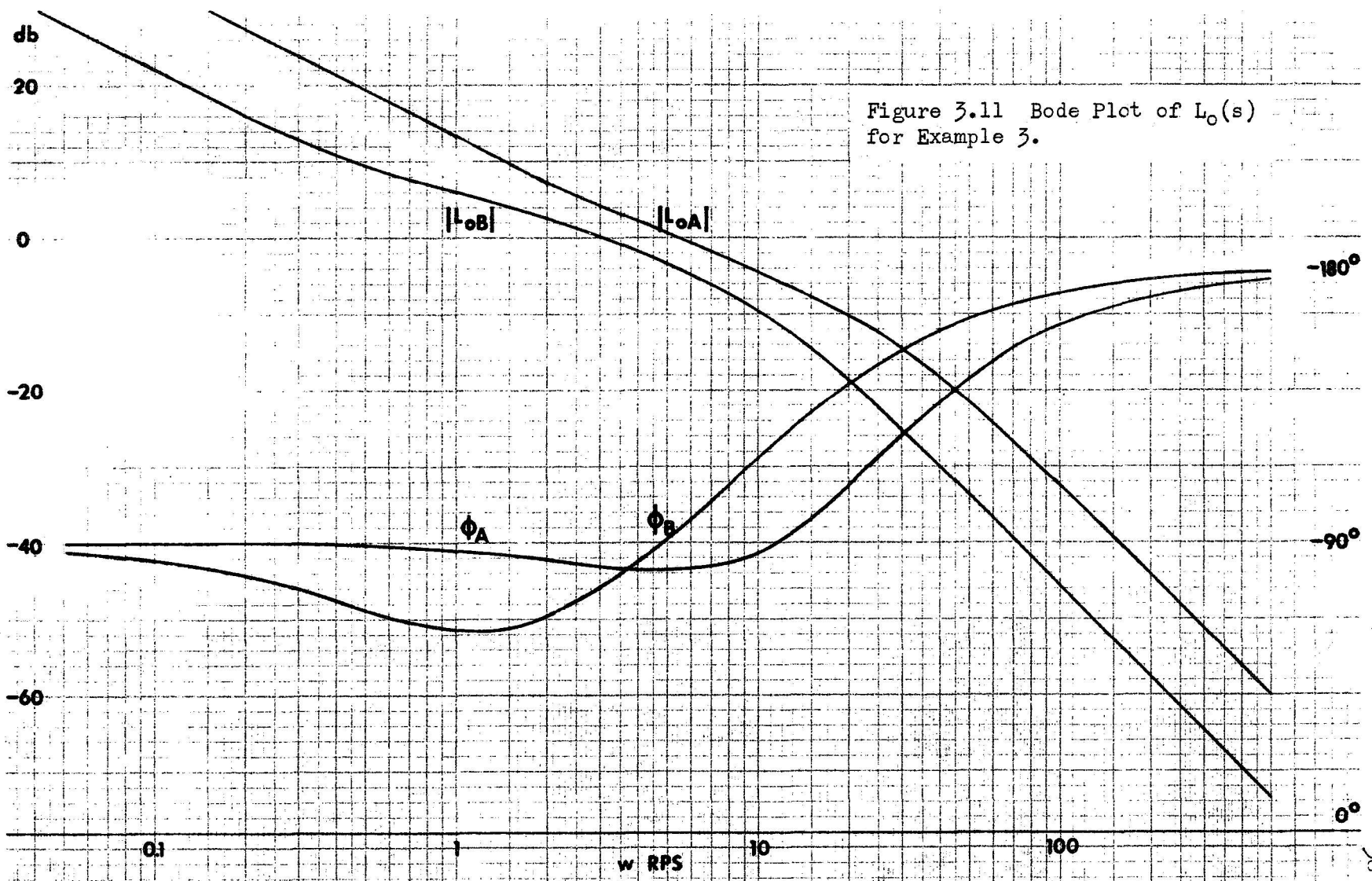


Figure 3.11 Bode Plot of $L_0(s)$ for Example 3.

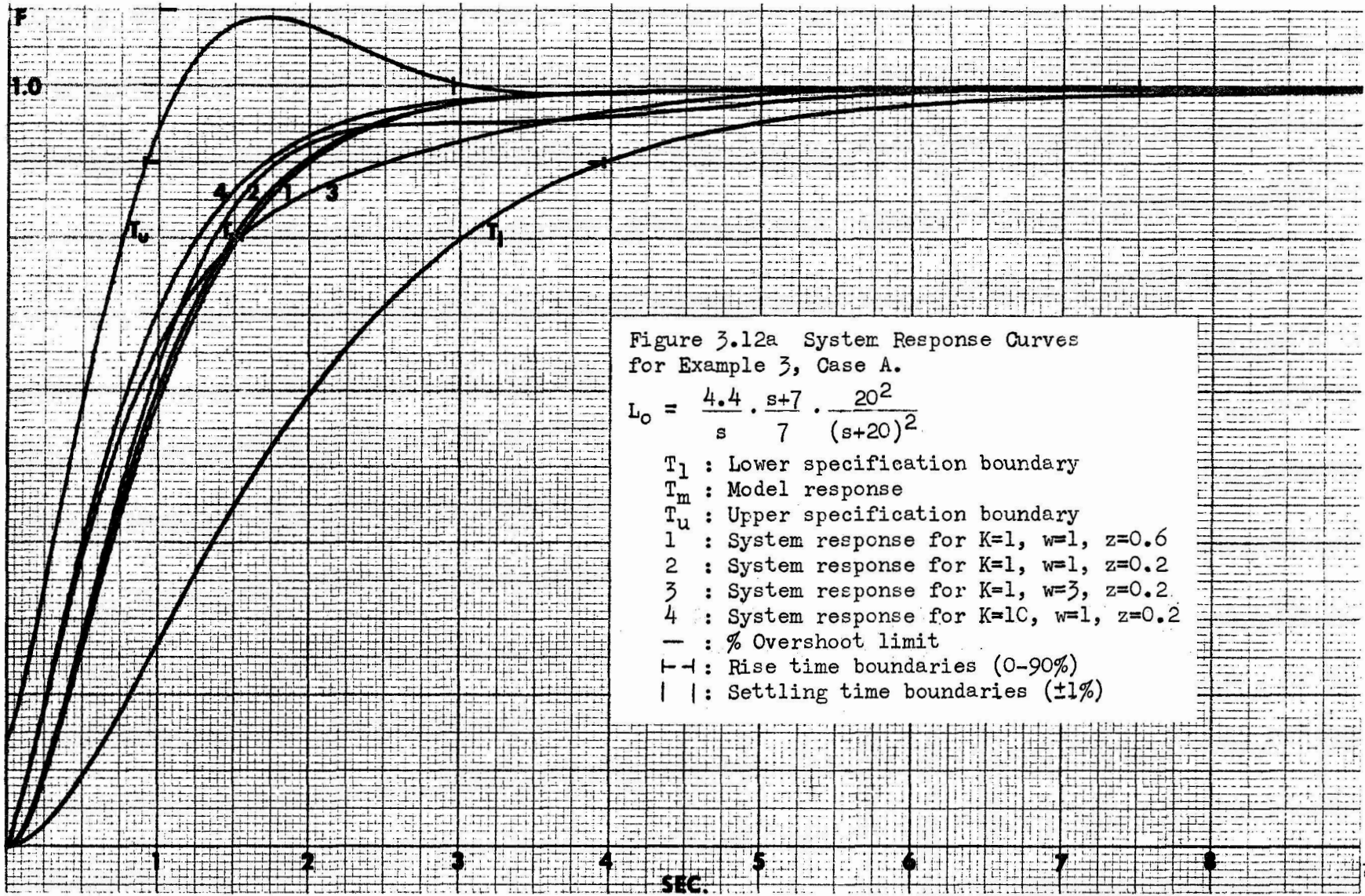
of L_{OA} (data obtained from figure 3.11), at the w_x frequencies selected, is well above the minimum $-L_O(jw_x)$ boundaries. Also, in this case the phase restriction of $w_x = 2$ rps is observed.

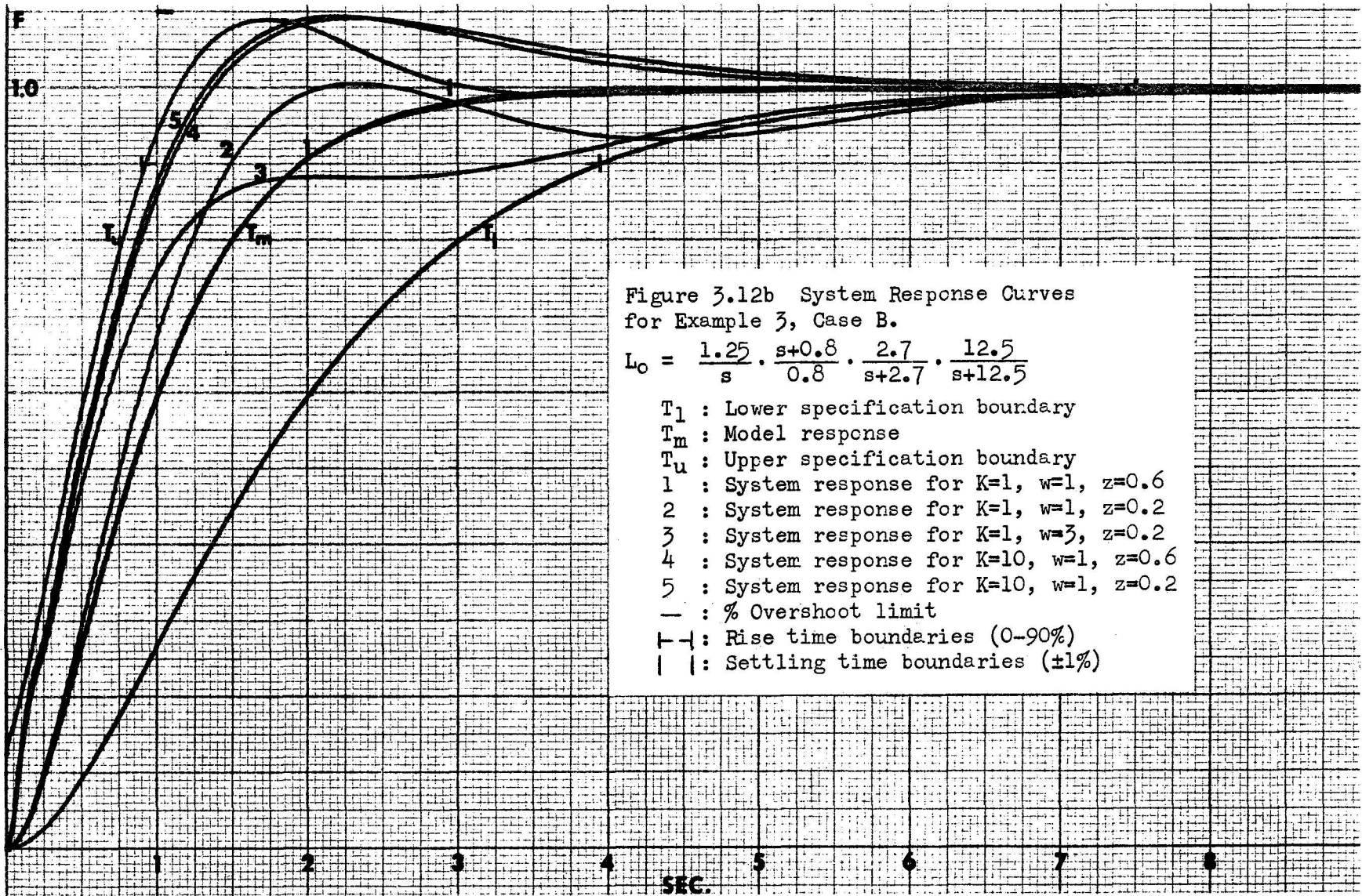
The ineffective use of allowable specification space suggest that a more economical design may be possible. This is attempted in case B. Observe that in case B, figure 3.12b, the response curves more effectively utilize the specification space. Referring to figure 3.10, it is seen that the actual location of L_{OB} , at the w_x frequencies selected, is fairly close to the minimum $-L_O(jw_x)$ boundaries due to T_u (left side), and that phase restrictions are ignored after $w = 1$. The design is more economical in terms of lower crossover and drop-off frequencies, i.e. in reduced bandwidth, as can be seen in figure 3.11.

Both design results are within the given specifications*, however, again, as in example 2, for minimum plant parameters the system response shows undershoot, response curve 2, figure 3.12b. This indicates a dominate third-order type system, see figure 3.7 and section 3.3 of example 2. It was thought that using a third-order model which more closely "models" the actual response might help eliminate this undershoot. This leads to example 4, in the next chapter.

Another reason a third-order model might be desired is that the $P(1/P_0)$ block in the verification model (section 1.6) might be

*Note that although curves 4 and 5 of figure 3.12b lie outside of the time response of T_u , shown for reference, that they still satisfy the three (gross) specifications given.





difficult to construct. If the two-degree-of-freedom system of example 1 (step 6, section 2.1) is desired, then $g(t)$ at $t = 0$ considerations require T_m to have at least one more excess pole than P_0 , or for the P_0 being used (second-order) T_m must be at least third-order (see discussion of step 1, example 1, section 2.1).

CHAPTER IV

THIRD-ORDER MODEL

4.1 Introduction

In the following example, the design shall attempt to control the undershoot type response for minimum plant parameters while meeting the same specification of example 3. It also illustrates the change in model requirements for a different choice of desired system configuration.

In example 3, the effects of over-design (conservative) was noted. In the following example, under-design shall be investigated to see if the system response then exceeds specifications.

4.2 Example 4, Third-order Model With 10% Allowable Overshoot

Given: Plant transfer function, $P(s) = kw^2/(s^2+2z_pw_p s+w_p^2)$

with parameter variations: $1 \leq k \leq 10$,

$$1 \leq w_p \leq 3,$$

$$0.6 \geq z_p \geq 0.2.$$

and desired time domain specifications as follows:

Rise time, 0 to 90% : 0.90 to 3.95 seconds

Settling time, $\pm 1\%$: 2.95 to 7.50 seconds

Overshoot limit : 10%

Step 1) Finding time specification boundaries.

The desired system configuration will be the two-degree-of-freedom system of example 1, (see section 2.1, step 1). Therefore T_1 must be at least a third-order transfer function. By investigating time response of transfer functions of the form

$T_1 = ab^2/(s+a)(s+b)^2$, it was found that $T_1 = 20/(s+1)^2(s+20)$,

satisfies the requirements: rise time = 3.95 seconds, settling time = 7.50 seconds, and 0% overshoot. Similarly, by investigating time responses of transfer function of the form

$$T_u = ac(s+d)(s+e)^2/de^2(s+a)(s^2+bs+c),$$

it was found that

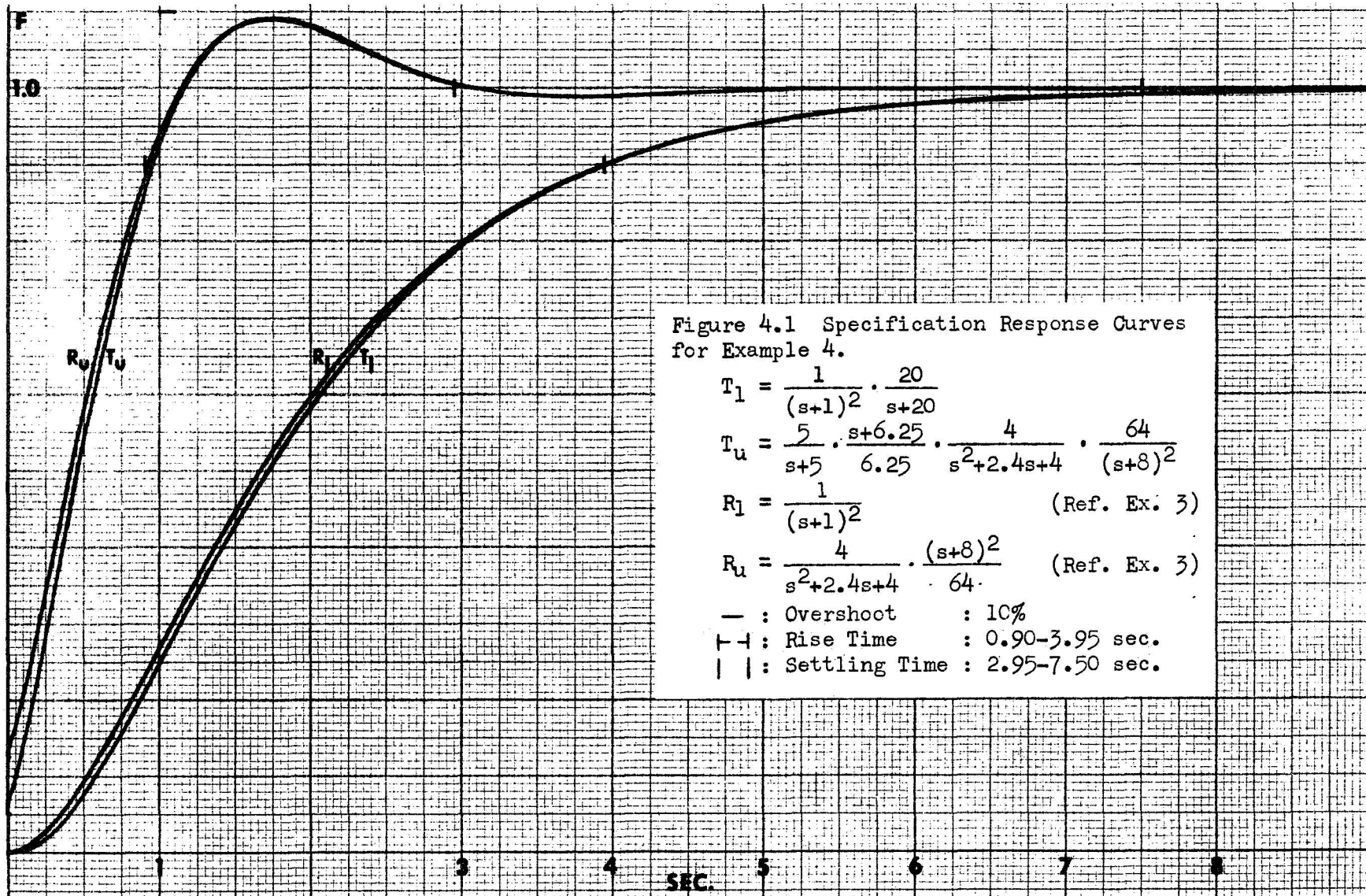
$$T_u = (5)(4)(s+6.25)(s+8)^2/(6.25)(64)(s+5)(s^2+2.4s+4),$$

approximately satisfies the requirements, rise time = 0.90 seconds, settling time = 2.95 seconds, and 10% overshoot. (The actual rise time of T_u is 0.95 seconds, or 0.05 seconds more than that specified as the minimum rise time, 0.90 seconds). The time response of these boundary transfer functions along with those of example three (for comparison) are shown in figure 4.1.

Step 2) Choosing T_m .

Careful examination of the system response curves of example 3B, figure 3.12b, shows that part of the reason for the undesirable response (undershoot) of curve 2 may be due to the relatively large rise and settling time allowed between the model transfer function time response curve T_m and the lower specification boundary transfer function time response curve T_1 . Figure 3.12b shows the allowable rise time between response curves T_u and T_m (measured along 90% line) is 1.05 seconds whereas between $T_m(t)$ and $T_1(t)$ is 2.00 seconds, and the allowable settling time between response curves T_u and T_m (measured along $\pm 1\%$ of 1.0 limits) is 0.35 seconds whereas between response curves T_m and T_1 is 4.20 seconds.

Note, however, that for approximately the first two seconds the response curves of the system lie between response curves T_u and T_m .



That is, the system initially responds between $T_u(t)$ and $T_m(t)$ but tends to reach steady-state between $T_m(t)$ and $T_1(t)$. It was felt that this could be contributing or allowing the poor system response. If the system could be made to react between response curves T_u and T_m , a more reasonable response might be obtained. This was attempted by choosing T_m closer to T_1 on the Bode plot, rather than near the center of the allowable area. This, at least, decreases the time between $T_m(t)$ and $T_1(t)$. T_m was not chosen equal to T_1 due to considerations mentioned in step 1, example 2 (section 3.2).

From the above considerations, the following model was picked.

$$T_m = (1.25)^2(25)/(s+1.25)^2(s+25). \text{ See figure 4.2.}$$

$\angle T_m/T_u$	$ T_m/T_u $	w_x rps	$ T_m/T_1 $	$\angle T_m/T_1$
-27.2°	.912	0.4	1.072	
-47°	.676	0.8	1.161	
-53°	.5755	1.0	1.23	
-54.5°	.327	2.0	1.413	
-78.84	.285	4.0	1.531	
	.214	8.0	1.585	
	.162	10.0	1.585	
	.0913	20.0	1.778	
	.00912	40.0	1.820	
	.001995	80.0	1.905	
	.0007245	100.0	1.995	
	.000955	200.0	1.995	

Table 4.1 Magnitude and Phase Ratios
for Example 4.

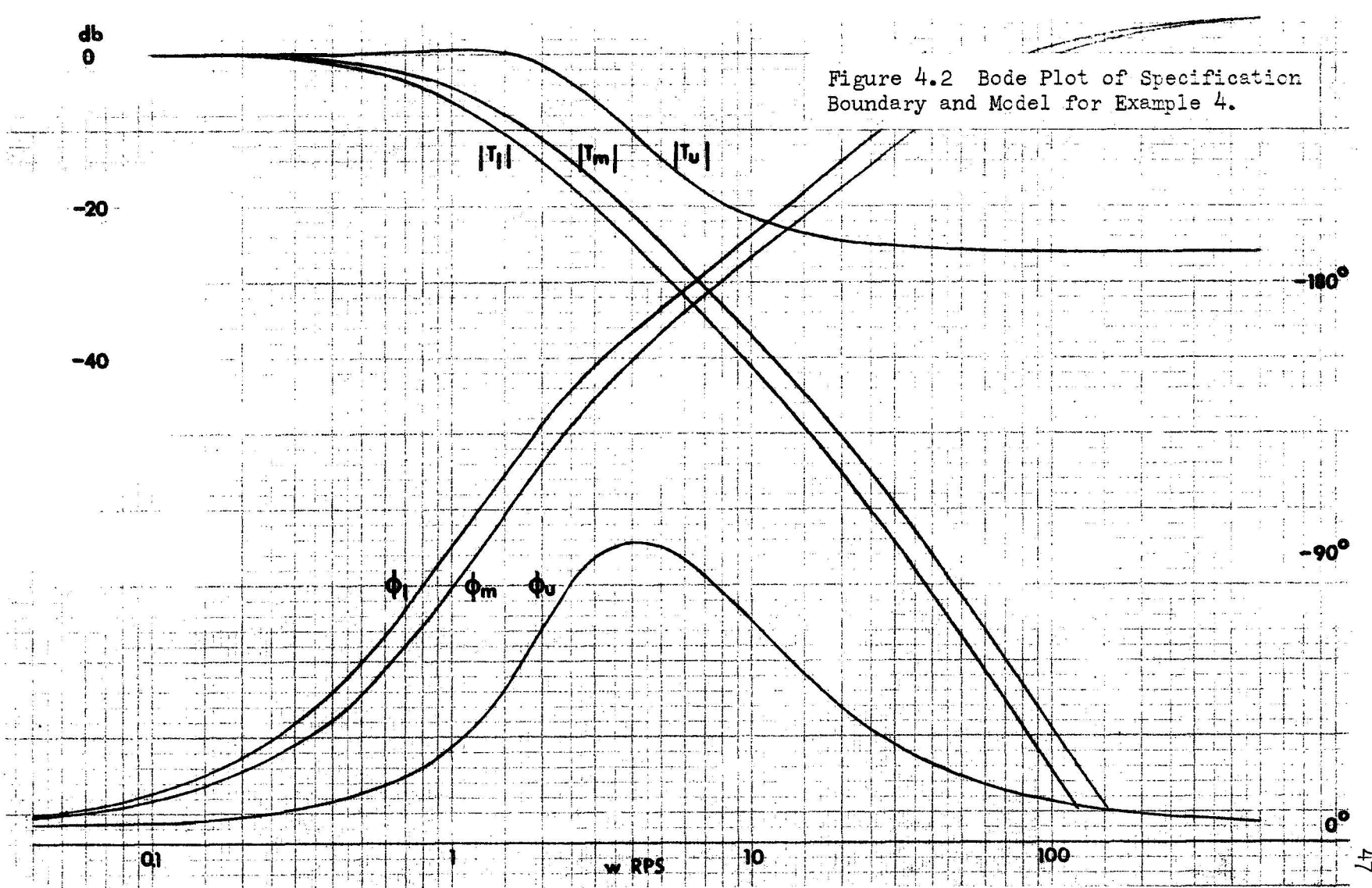


Figure 4.2 Bode Plot of Specification Boundary and Model for Example 4.

Step 3) Choosing $P_o(s)$. The same P_o used in example 2 was chosen. See reference {1} for details of method, appendix A for $P_o(jw_x)/P(jw_x)$ data, and figure 4.3 for resulting plot.

Steps 4 and 5) Determining loci of $-L_o(jw_x)$ minimum boundaries and feasible $L_o(jw)$ function. See design details given in reference {1}.

For this example, three different L_o 's were formed,

$$L_{oA} = (2)(20)(500^2)/s(s+20)(s+500)^2,$$

$$L_{oB} = (1.5)(15)(450)(740)/s(s+15)(s+450)(s+740), \text{ and}$$

$$L_{oC} = (0.28)(20.5)(400)(650)(s+0.15)/ \\ 0.15s(s+1)(s+20.5)(s+400)(s+650)$$

See figure 4.4

Note that the excess poles over zeros of the L_o 's ($e_L = 4$) are one more than that of T_m ($e_T = 3$) as required to have $h(t) = 0$ at $t = 0$, (see discussion of step 1, example 1, section 2.1).

The first loop transmission, L_{oA} , was an initial attempt. The second loop transmission, L_{oB} , is to determine the effects of under-design. The third loop transmission, L_{oC} , is an attempt at a more economical design.

Step 6) System configuration is the two-degree-of-freedom system of example 1 (step 6, section 2.1), so that

$$T = GP/(1+GPH) = T_m(1+L_o)P/(P_o+PL_o)$$

$$\text{or } T_A = T_m \left[\frac{((s^4 + 1020s^3 + 2.7 \times 10^5 s^2 + 5 \times 10^6 s + 10^7) kw^2 (s^2 + 1.2s + 1))}{((s^4 + 1020s^3 + 2.7 \times 10^5 s^2 + 5 \times 10^6 s) (s^2 + 2z_p w_p s + w_p^2) + 10^7 kw^2 (s^2 + 1.2s + 1))} \right]$$

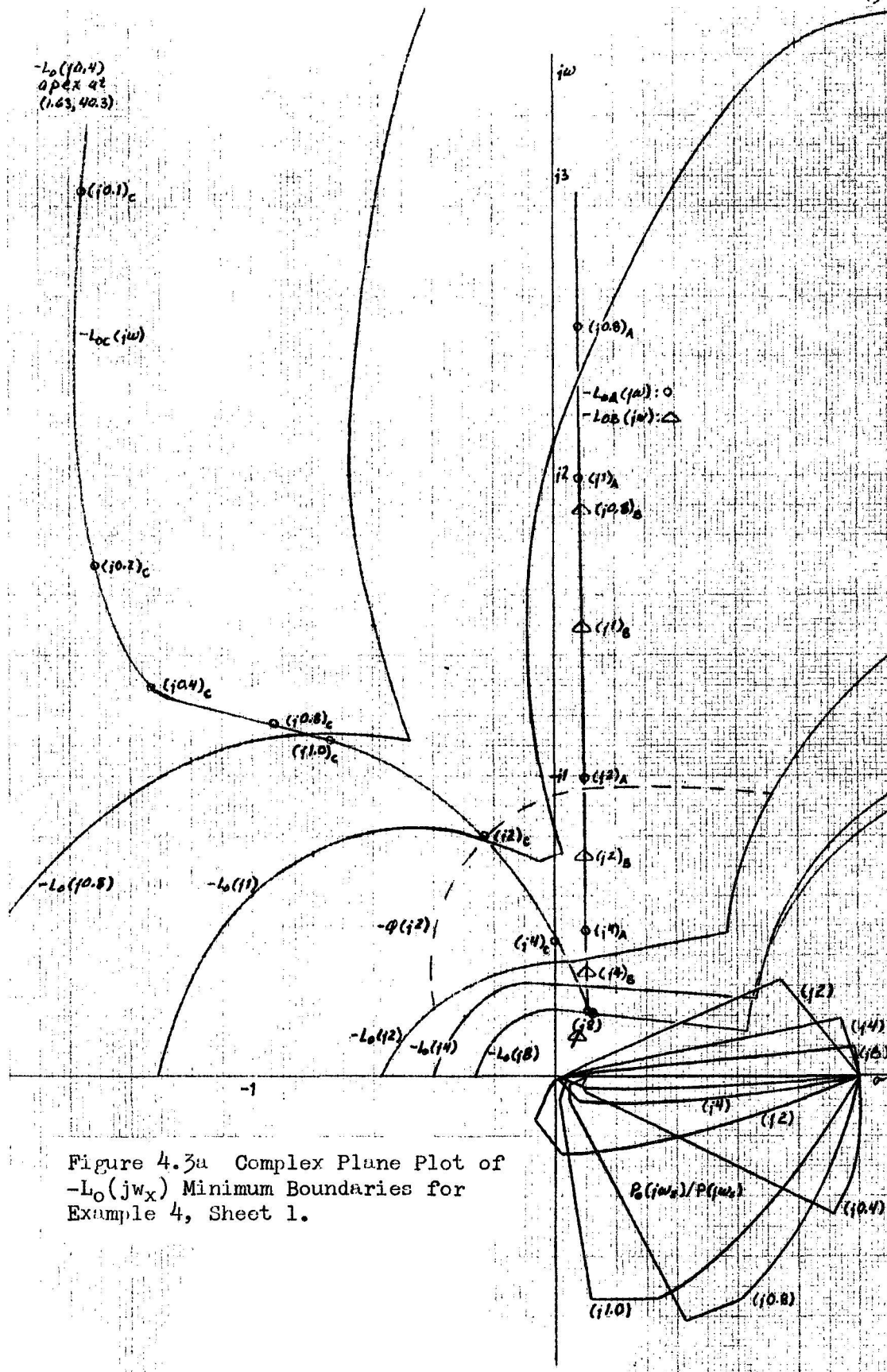
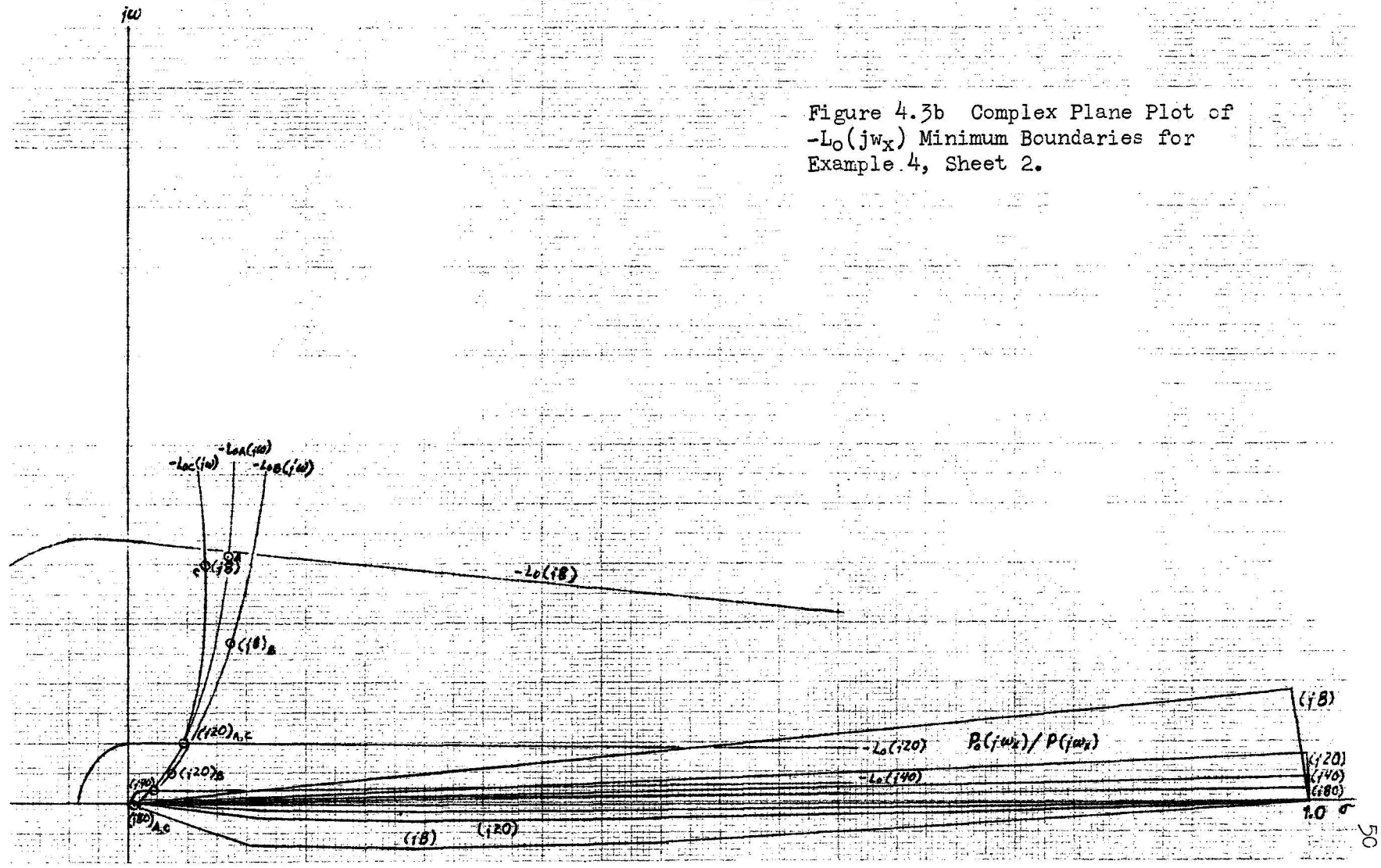


Figure 4.3a Complex Plane Plot of $-L_O(jw_X)$ Minimum Boundaries for Example 4, Sheet 1.

Figure 4.3b Complex Plane Plot of $-L_0(j\omega_x)$ Minimum Boundaries for Example 4, Sheet 2.



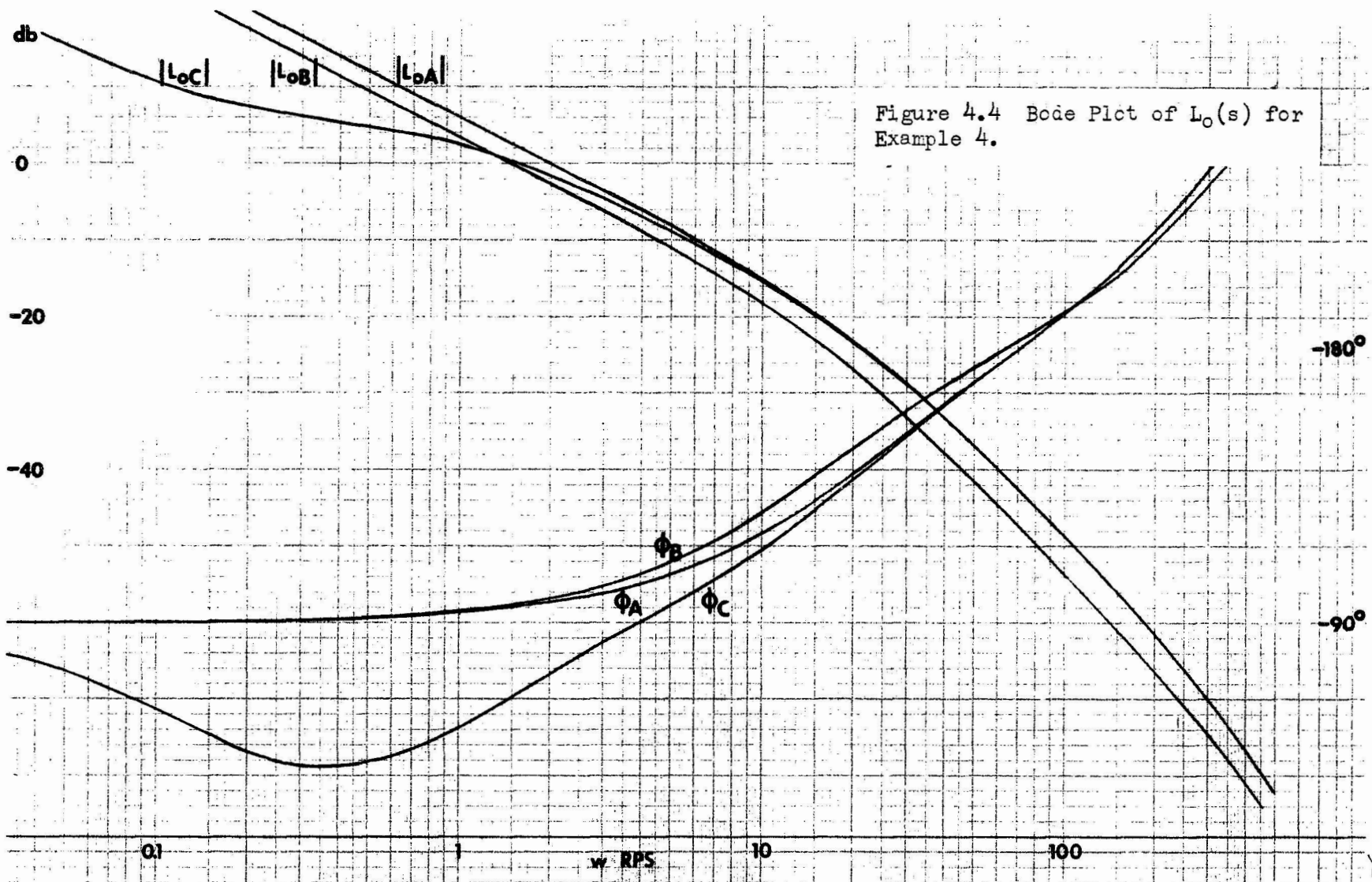


Figure 4.4 Bode Plot of $L_o(s)$ for Example 4.

$$T_B = T_m [(s^4 + 120.5s^3 + 3,085,000s^2 + 499,000s + 7492000) kw^2(s^2 + 1.2s + 1)] +$$

$$[(s^4 + 120.5s^3 + 3,085,000s^2 + 499,000s)(s^2 + 2z_p w_p s + w_p^2) +$$

$$7492500kw^2(s^2 + 1.2s + 1)]$$

$$T_C = T_m [(s^5 + 1071.5s^4 + 282595.5s^3 + 5611525s^2 + 15279333.33s + 1492400)$$

$$kw^2(s^2 + 1.2s + 1)] + [(s^5 + 1071.5s^4 + 282595.5s^3 + 5611525s^2 +$$

$$5.33 \times 10^6 s)(s^2 + 2z_p w_p s + w_p^2) + 9949333.33kw^2(s + 0.15)(s^2 + 1.2s + 1)]$$

$$\text{where } T_m = (39.0625) + (s^3 + 27.5s^2 + 64.0625s + 39.0625)$$

4.3 Analysis of Example 4, Third-order Model With 10% Allowable Overshoot

Case A. After drawing the magnitude and phase on the Bode plot, figure 4.4, the data for the design frequencies, w_x , were transferred to figure 4.3, for a check. It was found that the data points of $L_o(s)$ for w less than two lie below their boundaries. However, the system response curves, figure 4.5a, show that this choice of $L_o(s)$ is within specification except when the plant is near $K = 1$, $w = 1$, $z = 0.2$, where the rise time is just outside of specifications (by 0.05 seconds or less). The response for minimum plant parameters still has a slight flattening out effect. Note that the design is conservative in that a large amount of the allowable time response space (particularly the allowable overshoot) is not used.

Case B. In this case, the effect of under-design is sought. L_{oB} , lies just below L_{oA} (from 2.5 to 5 db). This roughly amounts to a lowering of the crossover frequency by one-half or a gain decrease of about 25%. See figure 4.4. Plotting the magnitude and phase data on figure 4.3, shows L_{oB} lies below the minimum $-L_o(jw)$

boundaries for all w_x 's used in the design. The system response curves, figure 4.5b, show the rise time is exceeded for $K = 1$, $w = 1$ to 3, $z = 0.2$, by 0.13 to 0.64 seconds. Hence, ignoring the $-L_0(jw)$ minimum boundaries does lead to a system response which exceeds the given specifications.

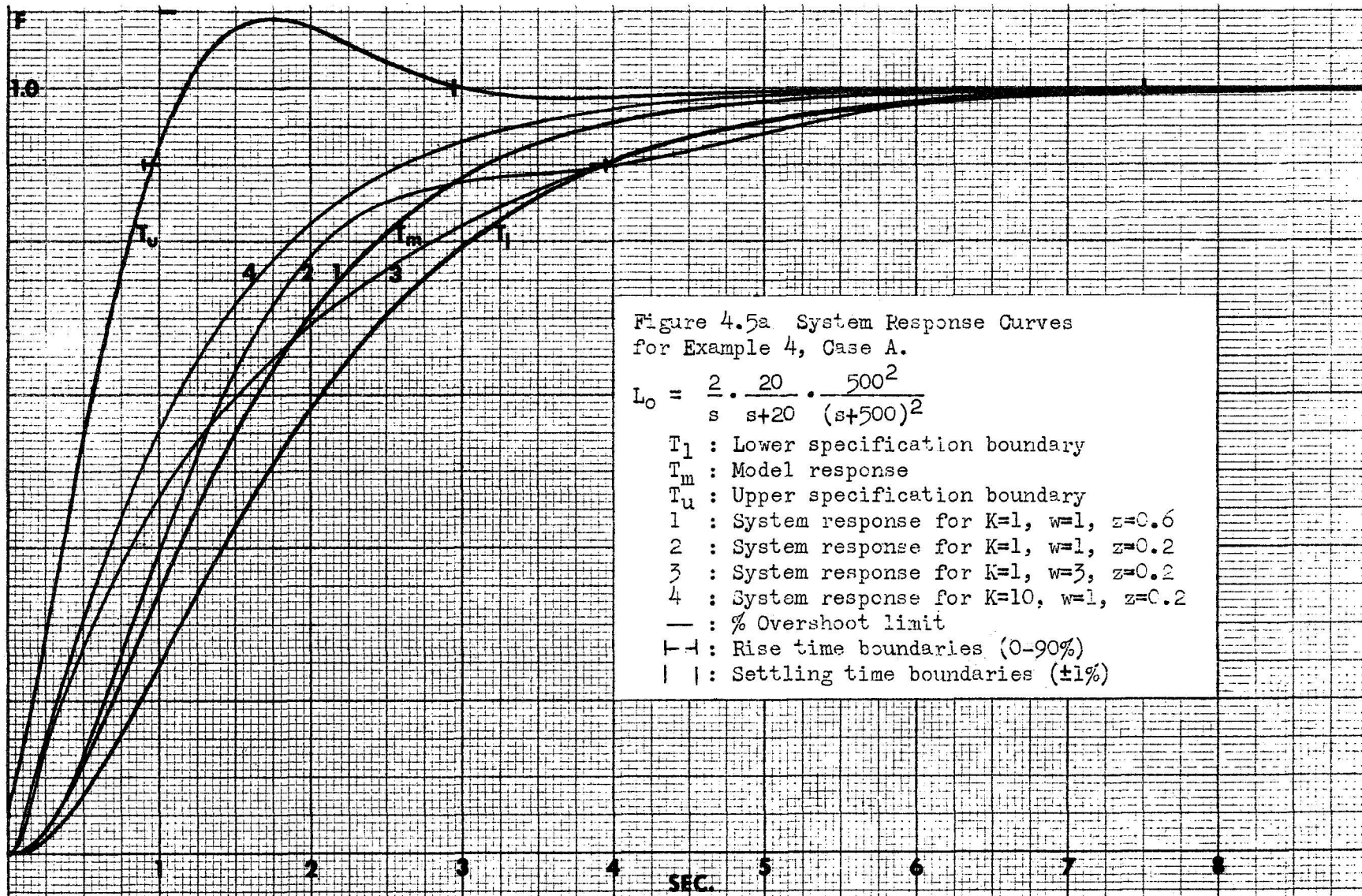
Case C. In Case A, the design did not fully utilize the allowable specification space (as shown by the time response curves, figure 4.5a), particularly with respect to overshoot. This case attempts to correct that and in so doing obtain a more economical design.

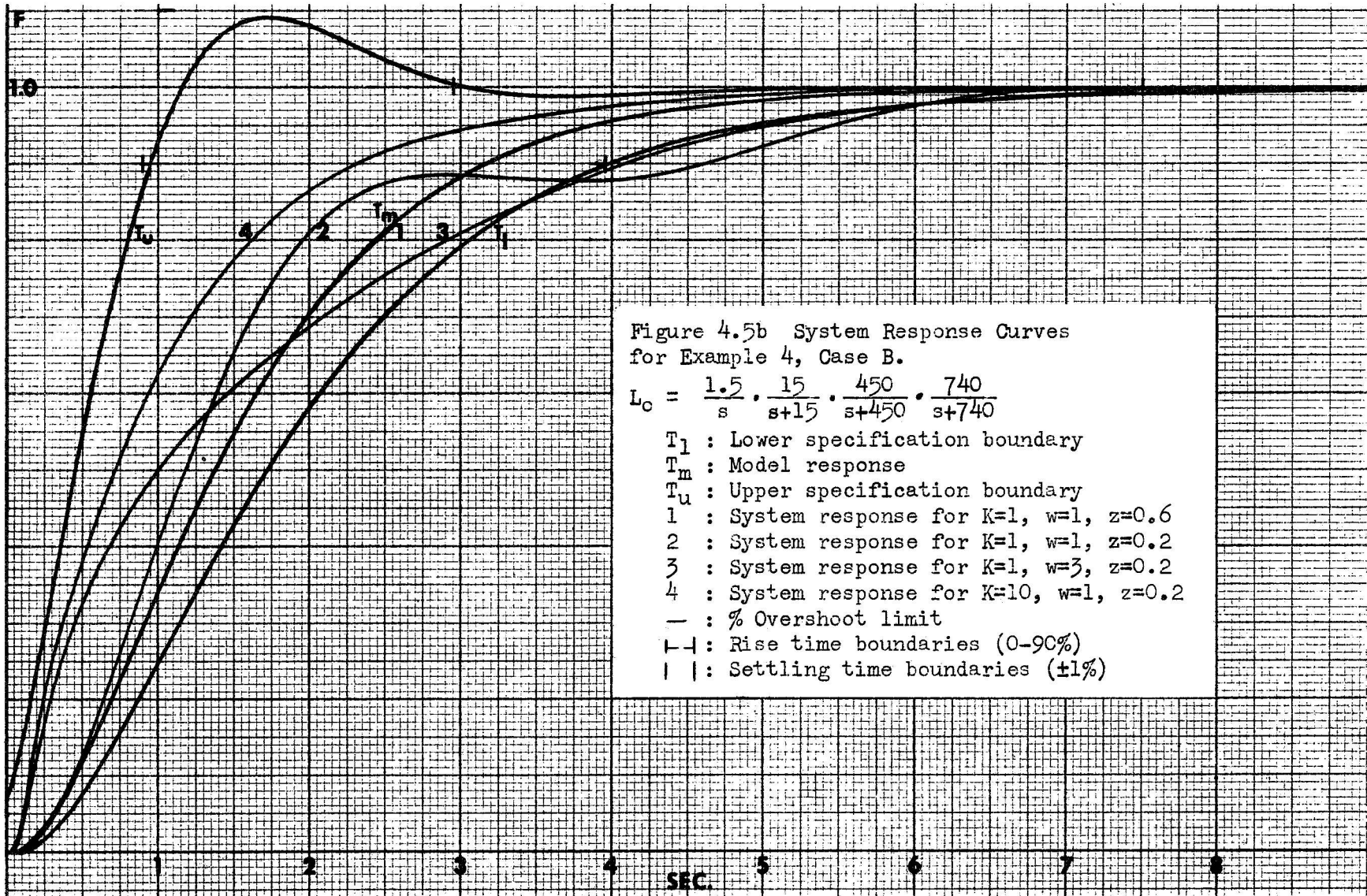
Note from Bode Plot figure 3.3, example 2 (no overshoot) (section 3.2) and figure 4.2 of this example, that the significant difference in T_u 's, due to overshoot, occurs for approximately one-half to twice the overshoot corner frequency, or for this case from $w = 1$ to 4 rps. Therefore, it seems reasonable that to fill the specification space, the design $L_0(s)$ should be as close as possible to the minimum $-L_0(jw)$ boundaries due to T_u , over this range. In trying to pick such an $L_0(s)$, it was found that the minimum boundary for $w_x = 0.4$ rps, in figure 4.3, could not be met. The relatively high gain required at $w_x = 0.4$ rps (12 to 16 db) means a pole must be introduced shortly thereafter to bring the magnitude down to the level required around $w_x = 1$ rps. But a pole introduces more phase lag, were less phase lag is needed (i.e. phase lead from -90° is required in the range $w_x = 0.4$ to 2 rps) which shifts the choice of $L_0(s)$ back to the right and away from the $-L_0(jw)$ boundaries due to T_u . Therefore the gain requirement at $w_x = 0.4$ rps must be ignored

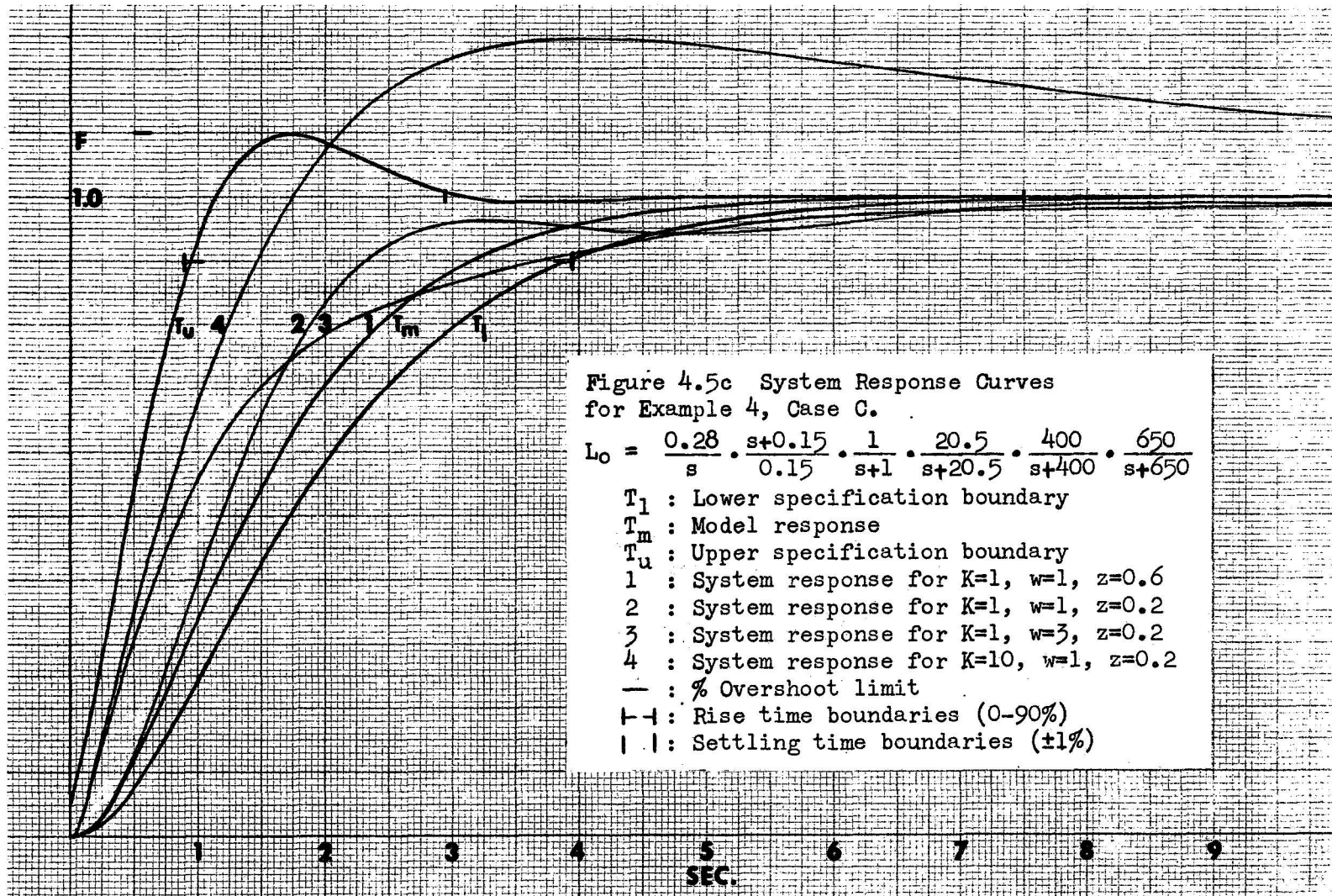
if it is desired to fit the $L_0(s)$ curve to the minimum boundaries due to T_u in the region of $w_x = 0.8$ to 8 rps. From the final value theorem of Laplace transform theory, it is suspected that the settling time and/or overshoot may be out of specification due to $L_0(jw)$ being so far from the $-L_0(j0.4)$ boundary.

The attempt to fill the specification space while ignoring the minimum levels for $w_x = 0.4$ rps, 0.2 rps, etc., (see figure 4.3) led to a system response which exceeds specifications, see figure 4.5c. In order to correct this, again either T_m and/or P_0 could be changed and a new design calculated. Observe, on figure 4.5c, that for the first couple of seconds the response is within specification, which could be roughly predicted by Laplace transform theory initial value theorem, although the specific change over from the domain of initial value theorem to the domain of final value theorem cannot be explicitly stated.

A comparison of response curves 2 of example 4 case C, figure 4.5c, with that of example 3 case B, figure 3.12b, shows that the undershoot was significantly reduced. This might tend to indicate that a dominant third-order model helped reduce the undershoot, except it was noticed that T_m is really not a dominant third-order transfer function, i.e. the pole is far-off ($s = -25$) and not close, as is necessary for a dominant type system. However, the improvement might be attributed to moving T_m closer to T_1 and thereby attaining a better P_0, T_m match. The design was terminated at this point, in order to investigate the dominant pole-zero design approach.







CHAPTER V

DOMINANT POLE-ZERO DESIGN

5.1 Purpose of Investigating a Dominant Pole-Zero Design

A dominant pole-zero design, using the specifications and plant of example 4, section 4.2, shall be performed in order to compare the results and see if any useful information can be gained with regard to eliminating the undershoot type response.

The design procedure is a recently improved technique developed by Horowitz [10]. The following results are shown so that the work can be checked, however, for details of the method see reference [10].

5.2 A Dominant Pole-Zero Design

Step 1) Determining the range of variation of plant on complex plane. For the given plant,

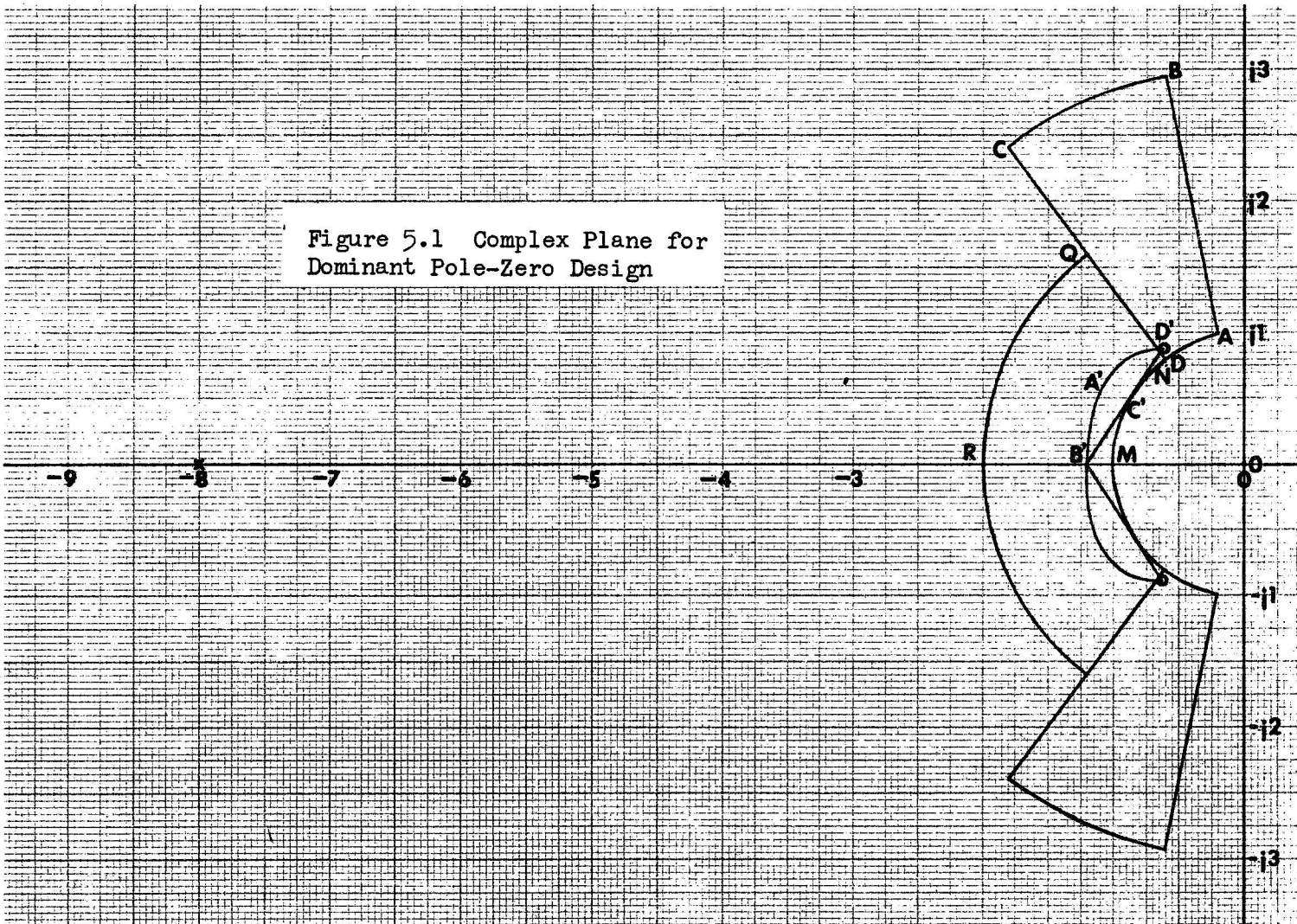
$$P = kw^2/(s^2+2z_pw_p s+w_p^2),$$

$$1 \leq K \leq 10, 1 \leq w_p \leq 3, 0.6 \geq z_p \geq 0.2$$

different values of the parameters were substituted into the equation and the resulting equation solved for s . For example, for $w = 1$, $z = 0.6$, $P/k = 1/(s^2+1.2s+1) = 1/(s+0.6+j0.8)(s+0.6-j0.8)$. The values of s were then plotted on the complex plane and the boundary determined, see figure 5.1 area ABCD.

Step 2) Determining the range of variation of acceptable response on the complex plane. Calculations similar to those of step 1, were performed for T_1 and T_u of example 4 (step 1, section 4.2). See figure 5.1 area MNQR. It must be noted that over damped solutions of higher frequencies will satisfy the actual given time specifications and hence increase the area of acceptable variations, particularly

Figure 5.1 Complex Plane for Dominant Pole-Zero Design



along the negative real-axis. Thus the design that is accomplished here is probably not the best possible from the method. However, the purpose here, is to gain information for correcting the design method of this research and so condition as similar to those previously used were attempted.

Also observe in figure 5.1, that the acceptable region of variation is tangent to the plant region of variation. Again, it just happened that this is so. The design procedure of Horowitz [10] is such as to allow the regions to overlap and hence this design is probably overly restrictive.

Step 3) Mapping acceptable region MNQR into X, Y plane.

Several rough calculations were made to determine a δ . It seemed that a δ of twelve would be sufficient so detailed calculations were performed on a desk calculator, using the following equations.

$$Y = (\delta X/P_r) + (P_r - \delta^2/P_r^2) \quad \text{and,}$$

$$Y = S_r(X - S_r) + \delta/(X - S_r)$$

where P_r and S_r are defined by,

$$T_d(s) = P_r p_f / (s^2 + S_r s + P_r)(s + p_f),$$

p_f is closest far-off pole and subscript d denote dominant part.

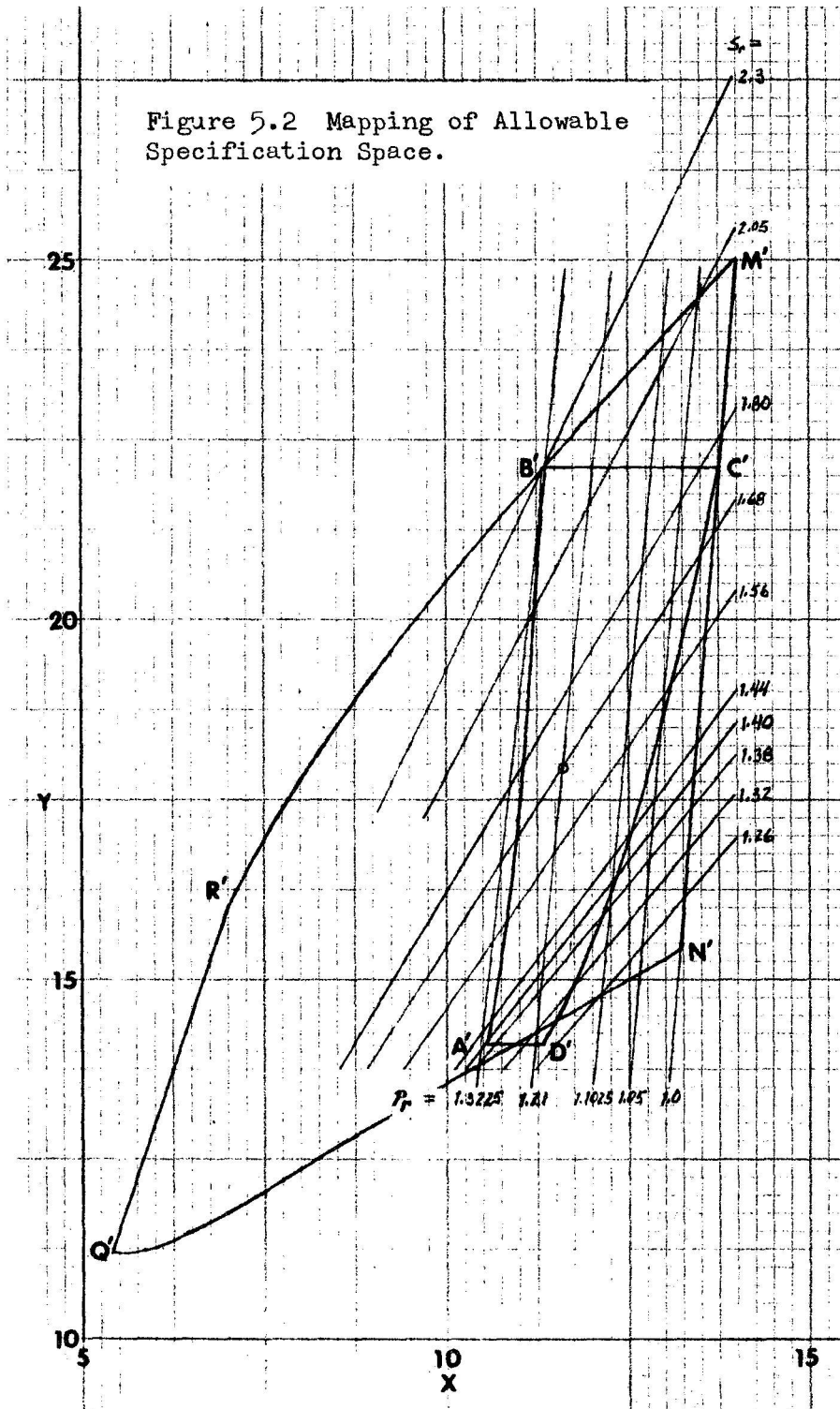
The range of variation of S_r and P_r were that of the acceptable region of $1 \leq P_r \leq 9$, $1.2 \leq S_p \leq 6$. The results are plotted on figure 5.2 and labeled MNQR.

Step 4) Mapping plant variation region ABCD into X, Y plane.

Mapping is accomplished by letting $X = S_p$ and $Y = P_p$, where

S_p and P_p are defined by

Figure 5.2 Mapping of Allowable Specification Space.



$$P \square k/s(s^2+sS_p+P_p); 0.4 \leq S_p \leq 3.6, 1 \leq P_p \leq 9$$

and mapping the region of $(s^2+sS_p+P_p)$. The results are plotted on figure 5.3 and labeled A'B'C'D'.

Step 5) Fitting A'B'C'D' into M'N'Q'R' and calculating dominant loop transmission.

A'B'C'D' was fitted into M'N'Q'R' as shown on figure 5.2. The points $X = 11.62$, $Y = 17.93$, $S_p = 1.45$, $P_p = 4.83$ were used as check points. Then (see {10})

$$X = S_p + kK = 1.45 + kK = 11.62 \Rightarrow kK = 10.17$$

$$P_o = \gamma/kK = 12/10.17 = 1.18$$

$$Y = P_p + kKS_o = 4.83 + 10.17S_o = 17.93 \Rightarrow S_o = 1.287$$

$$\begin{aligned} \text{and } L_d(s) &= kK(s^2+S_o s+P_o)/s(s^2+S_p s+P_p) \\ &= 10.1(s^2+1.29s+1.18)/s(s^2+S_p s+P_p) \end{aligned}$$

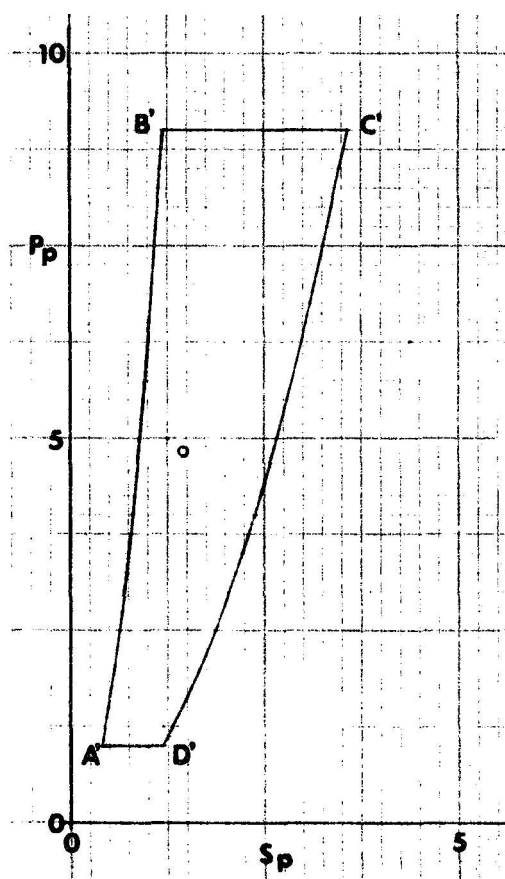
$$\text{Now } p_f = \frac{kKP_o}{P_r} = \frac{\gamma}{P_r} \quad \text{so } (p_f)_{\min} = \gamma/(P_r)_{\max} = 12/1.44 = 8.3$$

($\sqrt{P_r}$, max = 1.2 obtained from figure 5.1)

Step 6) Check of γ and determining far-off poles of $L(s)$. The Area A'B'C'D' of figure 5.2 was plotted onto figure 5.1 to check the angle of departure of the zeros of system dominant characteristic equation. A lag corner frequency at $w = 8$ was assumed, then the angle of departures checked for the A'B'C'D' boundary on figure 5.1, and found satisfactory.

Therefore, starting with $L = kK/s$ and $p_f = 8$, an average -9db/octave slope was assumed between w_{c1} and w_{c2} and $L(s)$ formed on the Bode plot, figure 5.4. w_{c2} was chosen as the point where

Figure 5.3 Mapping of Plant Variation Region



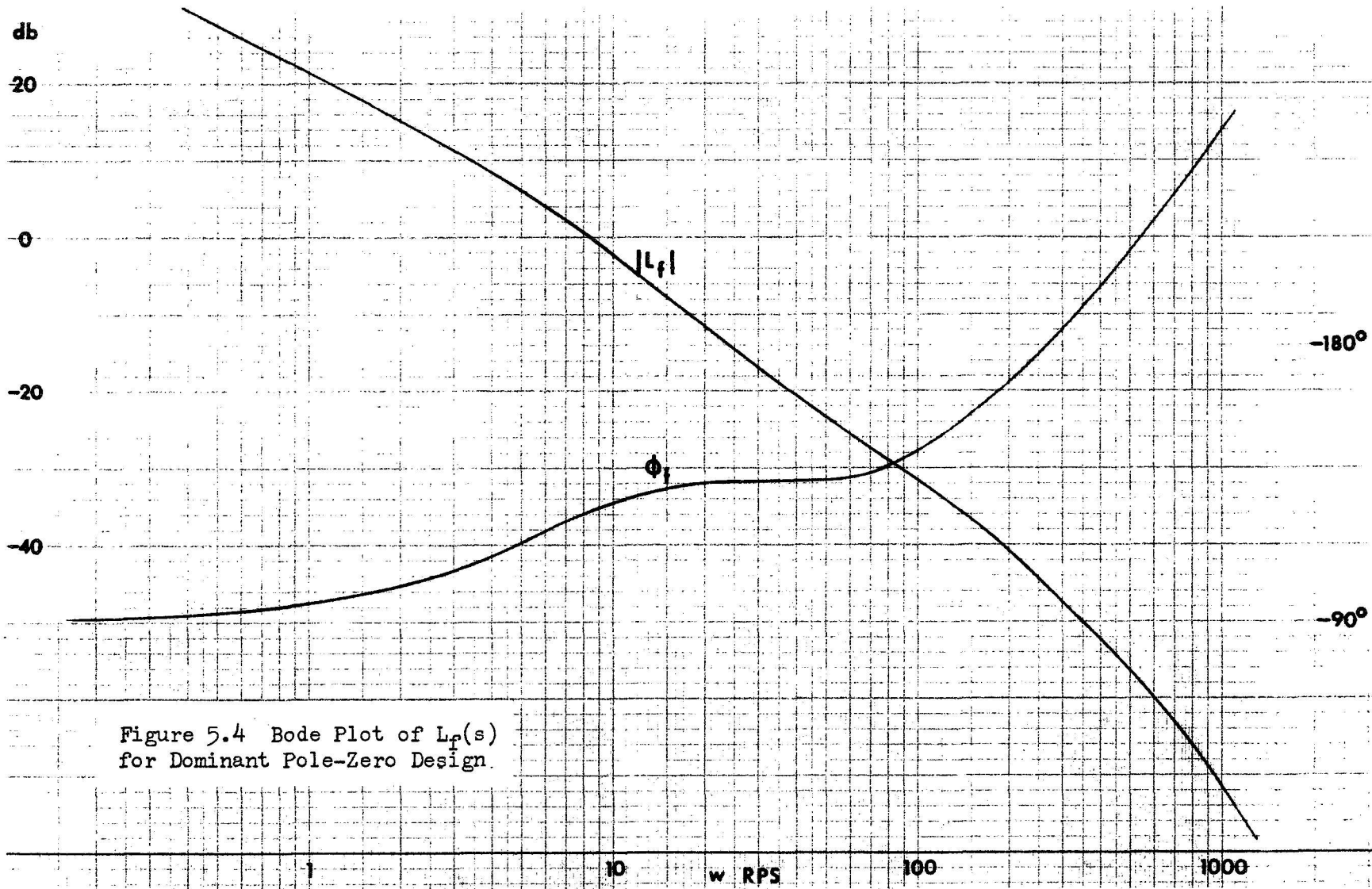


Figure 5.4 Bode Plot of $L_f(s)$ for Dominant Pole-Zero Design.

$L(s)$ crossed the $20 \log 90 = 39.1\text{db}$ line (kw_{\max}^2 of example 4, section 4.2, is 90). The result is

$$L(s) = [12kw^2(s^2+1.29s+1.18)/1.18s(s^2+2z_pw_p s+w_p^2)] \times \\ [(8)(160)(800)(2000)(s+32)/32(s+8)(s+160)(s+800)(s+2000)]$$

Step 7) System Configuration:

The two-degree-of-freedom system of example 4 (step 6, section 2.1) is desired. From {10},

$$G(s) = r(s)/d_f^{\#}(s)$$

$$\text{and } H(s) = K(s^2+sS_o+P_o)n_f/d'(s)r(s)$$

where $r(s)$ can be dominant fixed poles and zeros to satisfy

specifications other than response in acceptable region
(not used)

$d_f^{\#}(s)$ is the far-off poles added to L to simplify G ,

$d_f^{\downarrow}(s)$ is the far-off poles of L , and

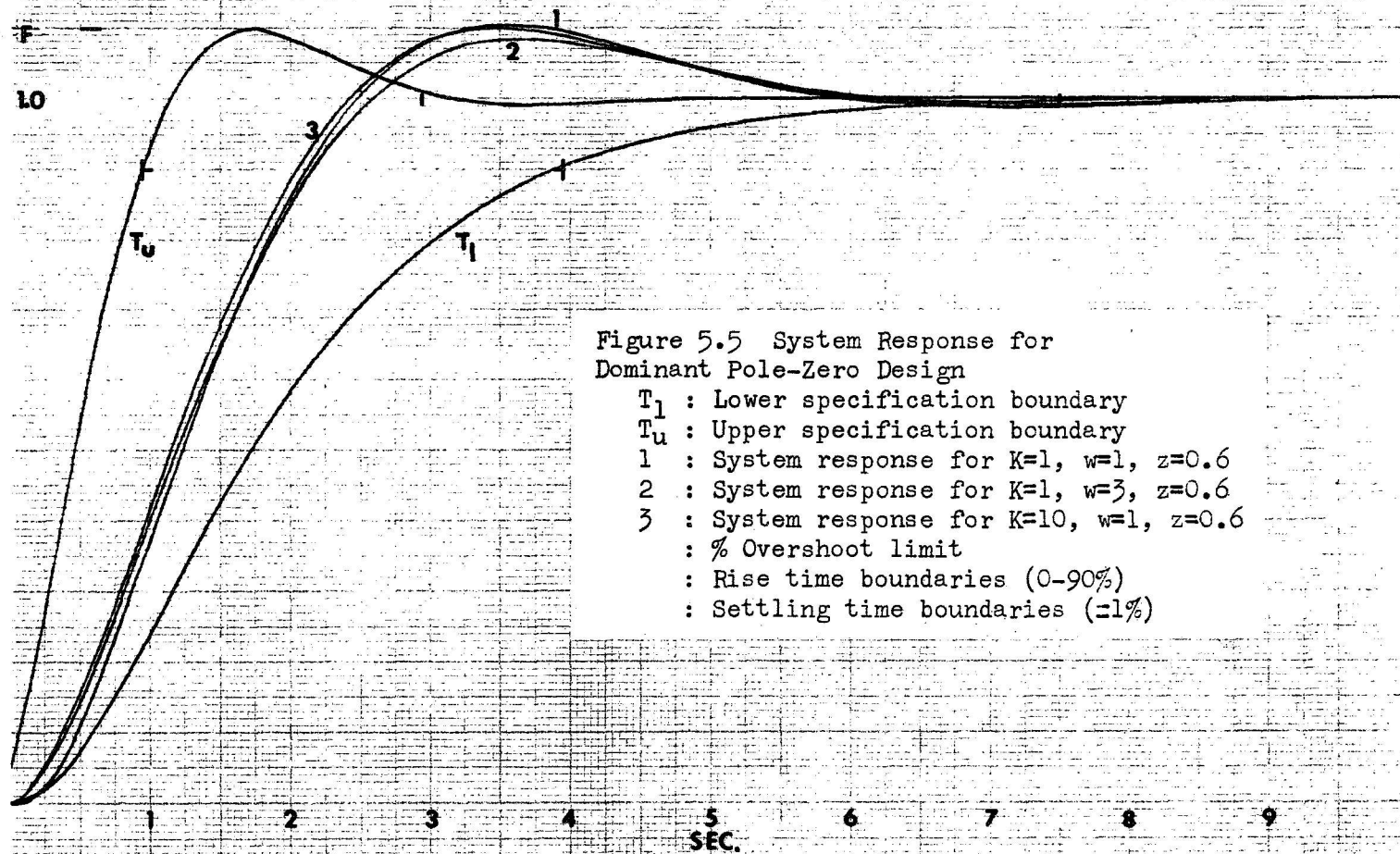
$n_f(s)$ is the far-off zeros of L

or $G = 1$, $H = L$

5.3 Results of Dominant Pole-Zero Design

The system response, figure 5.5, shows a closely grouped set of responses (only limiting cases were shown) pretty much centered in the allowable specification space. No undershoot was noted. Needless to say, the specifications are satisfied.

A look at the dominant pole-zero pattern of the transfer function, figure 5.6, shows a very simple pattern. The only notable feature is that the pole from the origin (of L) has moved past the zero at $s = -8$. That is, there is no pole between the complex pair of poles and the first zero of the transfer function.



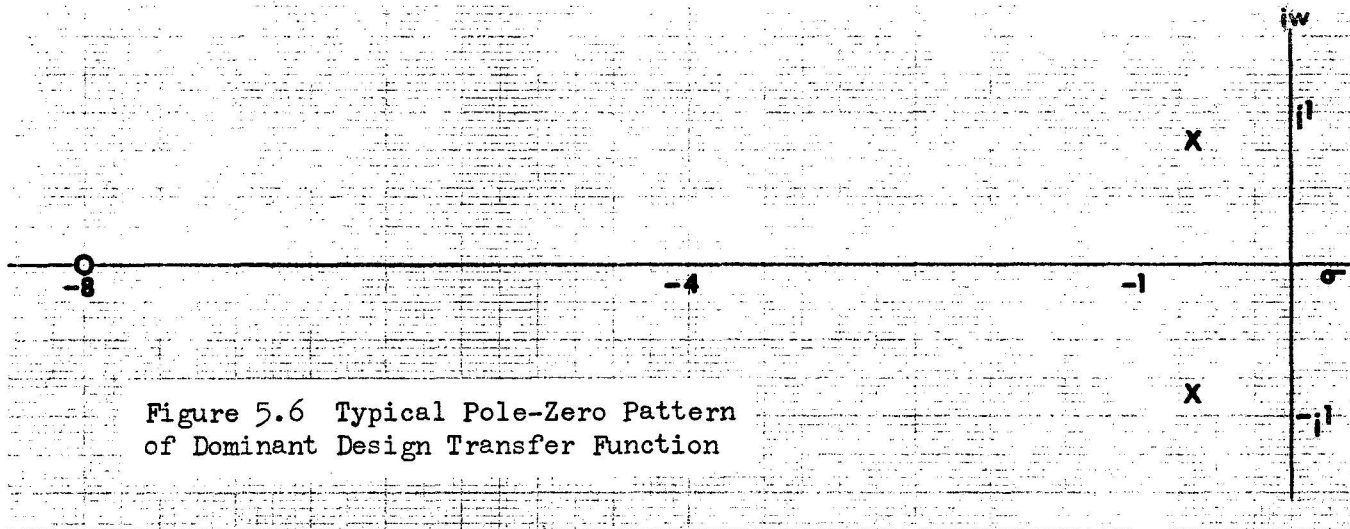


Figure 5.6 Typical Pole-Zero Pattern of Dominant Design Transfer Function

However, this was previous noted (section 3.3) as the probable cause of the undershoot. Therefore, this design investigation was of limited value in trying to determine trouble spots of the frequency method.

CHAPTER VI

CONCLUSION

6.1 Final Analysis

Comparison of the gain crossover frequencies of the final design of examples 3 and 4 figures 3.11 and 4.2, shows that the higher order model (example 4, section 4.1) resulted in a lower gain crossover frequency of approximately one half the previous value. It is suspected that higher order models will result in a lower gain crossover frequency with a resultant increase in the complexity of the system. It is also suspected that a point of diminishing returns will be reached either in terms of increased complexity (Compare transfer functions of step 6, sections 3.4 and 4.2) or in terms of significant decrease in gain crossover frequency.

In each of the multiple design examples (examples 3 and 4) it was found that the most economical design, in terms of lower crossover and drop off frequencies, was the one that most fully utilized the allowable specification space. That is, for a given $-L_0(j\omega)$ minimum boundaries map, a best design exists, but at present it seems a matter of trial and error to find it. However, by keeping in mind the points brought out by the previous investigation, such as having $L_0(s)$ intersect the boundaries due to T_u and following the minimum levels as closely as possible in the regions of significant change (due to change in requirements, such as allowing overshoot) in the Bode plot, a reasonable design may be obtain.

If a particular $-L_0(j\omega)$ minimum boundaries map leads to particularly difficult or impossible requirements on $L_0(s)$, the system transfer function model, T_m , and/or nominal plant, P_0 , can be

relocated or changed to yield a better map. Note that when the plant is at its nominal value, the system response is that of T_m . In this paper, the nominal plant, P_0 , was picked as the smallest value of the plant, so that any plant variations was above or from the nominal value. Therefore, in the examples the different system responses due to plant parameter variations, at least initially, was from $T_m(t)$ towards $T_u(t)$. If the nominal plant value is picked so that variation are around it rather than just above it, then it is suspected that the system response would be about $T_m(t)$. This was not tried in this paper due to the difficulty in arriving at a satisfactory scale for the complex plane $-L_0(jw_x)$ minimum boundaries map.

It must be stressed that computer (either analog or digital) verification of the results seems to be an intergal part of this design method, as nothing was noted that would predict the nature of the response. For example, the response might be damped oscillations within the time specification boundaries. When properly executed, this procedure does predict a design which satisfies at least the three parameters checked, i.e. rise time, settling time, and overshoot, and (at least in the examples) tends to follow the response of the model.

The preceeding investigation shows that time domain specifications can be translated to frequency domain specifications via specification modeling, at least for the "Frequency Response Approach to the Sensitivity Problem" design method presented in reference [1]. The procedure entails picking models which bound the time domain specifications and transfer these specifications to the frequency

domain. Then picking a model of the desired nominal system response. And finally, forming a nominal loop transmission, which initially may seem to be more art than technique, but with practice becomes readily apparent.

From this investigator's viewpoint, it seems that the modeling technique should work whenever it is desired to translate from the time domain to the frequency domain, however much investigation is yet to be done in this area.

BIBLIOGRAPHY

- {1} I. M. Horowitz, Synthesis of Feedback Systems, Academic Press, Inc., New York, N. Y., 1963, Section 6.7, Philosophy of the Frequency Response Approach to the Sensitivity Problem, pg. 267, and section 6.8 Realization of Sensitivity Specification Frequency Response Method, pg. 271.
- {2} Ibid, Section 6.9 Cost of Feedback, and Comparison of Two-Degree-of-Freedom Structures, pg. 280.
- {3} Ibid, Section 6.1 Configuration with Two-Degrees-of-Freedom, pg. 246.
- {4} Ibid, Section 5.17 Relative Merits of Open-loop Frequency Response Method and the T(s) Pole-zero Method, pg. 220, and section 5.18 the Price That Is Paid for a Dominant Type T(s), pg. 221.
- {5} Ibid, Section 5.10 Correlation between System Frequency Response and Time Response, pg. 188.
- {6} C. R. Wylie, Jr., Advanced Engineering Mathematics, Third Edition, McGraw-Hill, New York, 1966, pg. 242.
- {7} See 1, pg. 230 to 232, for example of time response curves.
- {8} C. L. Johnson, Analog Computer Techniques, Second Edition, McGraw-Hill, New York, 1963, pg. 84 to 86.
- {9} See 1, pg. 274, for discussion of choosing nominal $P_0(j\omega)$ as minimum $P(j\omega)$.
- {10} I. M. Horowitz, Optimum Linear Adaptive Design of Dominant Type Systems with Large Parameter Variations, (to be published, IEEE Trans. Automatic Control, 1969).

APPENDIX A

$P_o(jw_x)/P(jw_x)$ DATA FOR SECOND-ORDER PLANT

Determining P_o/P area of variation on complex plane for

$$\frac{P_o(jw_x)}{P(jw_x)} = \frac{s^2 + 2z_p w_p s + w_p^2}{k w_p^2 (s^2 + 1.2s + 1)} \quad s = jw_x$$

w_x rps	w_p rps	z_p	kP_o/P	
0.4	1.0	0.2	0.8359 - j0.2872	
		0.6	1.0000 - j0.0000	
	1.2	0.2	0.8661 - j0.3362	
		0.6	0.0028 - j0.0969	
	1.5	0.2	0.8883 - j0.3863	
		0.6	0.9977 - j0.1892	
	2.0	0.2	0.9026 - j0.4205	
		0.6	0.9846 - j0.2769	
	3.0	0.2	0.9088 - j0.4558	
		0.6	0.9635 - j0.3601	
	0.8	1.0	0.2	0.4155 - j0.2192
			0.6	1.0000 - j0.0000
1.2		0.2	0.4338 - j0.4160	
		0.6	0.9208 - j0.2334	
1.5		0.2	0.4399 - j0.5805	
		0.6	0.8295 - j0.4343	
2.0		0.2	0.4338 - j0.7123	
		0.6	0.7260 - j0.6027	
3.0		0.2	0.4155 - j0.8118	
		0.6	0.6104 - j0.7387	
1.0		1.0	0.2	0.3333 - j0.0000
			0.6	1.0000 - j0.0000
	1.2	0.2	0.2778 - j0.2546	
		0.6	0.8333 - j0.2546	
	1.5	0.2	0.2222 - j0.4629	
		0.6	0.6667 - j0.4629	
	2.0	0.2	0.1667 - j0.6296	
		0.6	0.5000 - j0.6296	
	3.0	0.2	0.1111 - j0.7407	
		0.6	0.3333 - j0.7407	

w_x rps	w_p rps	z_p	kP_o/P	
2.0	1.0	0.2	0.7398 + j0.3252	
		0.6	1.0000 - j0.0000	
	1.2	0.2	0.4695 + j0.1537	
		0.6	0.6875 - j0.1175	
	1.5	0.2	0.2445 + j0.0181	
		0.6	0.4185 - j0.1987	
	2.0	0.2	0.0651 - j0.0813	
		0.6	0.1953 - j0.2444	
	3.0	0.2	-0.0709 - j0.1445	
		0.6	0.0172 - j0.2529	
	4.0	1.0	0.2	0.9380 + j0.1935
			0.6	1.0000 - j0.0000
1.2		0.2	0.6410 + j0.1150	
		0.6	0.7200 - j0.0462	
1.5		0.2	0.3910 + j0.0538	
		0.6	0.4320 - j0.0753	
2.0		0.2	0.1970 + j0.0097	
		0.6	0.2240 - j0.0871	
3.0		0.2	0.0574 - j0.0172	
		0.6	0.0780 - j0.0817	
8.0		1.0	0.2	0.9849 + j0.0993
			0.6	1.0000 - j0.0000
	1.2	0.2	0.6802 + j0.0613	
		0.6	0.6929 - j0.0189	
	1.5	0.2	0.4307 + j0.0318	
		0.6	0.4409 - j0.0344	
	2.0	0.2	0.2365 + j0.0106	
		0.6	0.2440 - j0.0390	
	3.0	0.2	0.0973 - j0.0021	
		0.6	0.1024 - j0.0352	
	20.0	1.0	0.2	0.9976 + j0.0400
			0.6	1.0000 - j0.0000
1.2		0.2	0.6922 + j0.0249	
		0.6	0.6942 - j0.0084	
1.5		0.2	0.4423 + j0.0132	
		0.6	0.4439 - j0.0134	
2.0		0.2	0.2478 + j0.0049	
		0.6	0.2490 - j0.0150	
3.0		0.2	0.1089 - j0.0001	
		0.6	0.1097 - j0.0135	

w_x rps	w_p rps	z_p	kP_o/P
40.0	1.0	0.2	0.9994 + j0.0200
		0.6	1.0000 - j0.0000
	1.2	0.2	0.6939 + j0.0125
		0.6	0.6944 - j0.0042
	1.5	0.2	0.4439 + j0.0067
		0.6	0.4443 - j0.0067
2.0	0.2	0.2495 + j0.0025	
	0.6	0.2498 - j0.0075	
3.0	0.2	0.1106 - j0.0000	
	0.6	0.1108 - j0.0067	
80.0	1.0	0.2	0.9998 + j0.0100
		0.6	1.0000 - j0.0000
	1.2	0.2	0.6943 + j0.0063
		0.6	0.6944 - j0.0021
	1.5	0.2	0.4443 + j0.0033
		0.6	0.4444 - j0.0033
2.0	0.2	0.2499 + j0.0012	
	0.6	0.2499 - j0.0038	
3.0	0.2	0.1110 - j0.0000	
	0.6	0.1110 - j0.0033	
200.0	1.0	0.2	0.9999 + j0.0040
		0.6	1.0000 - j0.0000
	1.2	0.2	0.6944 + j0.0025
		0.6	0.6944 - j0.0008
	1.5	0.2	0.4444 + j0.0013
		0.6	0.4444 - j0.0013
2.0	0.2	0.2500 + j0.0005	
	0.6	0.2500 - j0.0015	
3.0	0.2	0.1111 - j0.0000	
	0.6	0.1111 - j0.0013	